Learning particle swarming models from data with Gaussian processes

Jinchao Feng* Charles Kulick † Yunxiang Ren ‡ Sui Tang §

March 8, 2023

arXiv:2106.02735v4 [stat.ML] 7 Mar 2023

Abstract

Interacting particle or agent systems that exhibit diverse swarming behaviors are prevalent in science and engineering. Developing effective differential equation models to understand the connection between individual interaction rules and swarming is a fundamental and challenging goal. In this paper, we study the data-driven discovery of a second-order particle swarming model that describes the evolution of N particles in $\mathbb{R}^d$ under radial interactions. We propose a learning approach that models the latent radial interaction function as Gaussian processes, which can simultaneously fulfill two inference goals: one is the nonparametric inference of the interaction function with pointwise uncertainty quantification, and the other is the inference of unknown scalar parameters in the non-collective friction forces of the system. We formulate the learning problem as a statistical inverse learning problem and introduce an operator-theoretic framework that provides a detailed analysis of recoverability conditions, establishing that a coercivity condition is sufficient for recoverability. Given data collected from M i.i.d trajectories with independent Gaussian observational noise, we provide a finite-sample analysis, showing that our posterior mean estimator converges in a Reproducing Kernel Hilbert Space norm, at an optimal rate in M equal to the one in the classical 1-dimensional Kernel Ridge regression. As a byproduct, we show we can obtain a parametric learning rate in M for the posterior marginal variance using L^∞ norm and that the rate could also involve N and L (the number of observation time instances for each trajectory) depending on the condition number of the inverse problem. Numerical results on systems that exhibit different swarming behaviors demonstrate efficient learning of our approach from scarce noisy trajectory data.We provide numerical results on systems exhibiting different swarming behaviors, highlighting the effectiveness of our approach in the scarce, noisy trajectory data regime.

1 Introduction

Swarming behaviour exhibited by interacting particles is very common, referring to particles of similar size aggregating together, milling about the same spot, moving en masse, or migrating in some direction. Examples include the aggregation of popular opinion on events, the flocking of birds, the schooling of fish, and the coordinated movement of robots. It is a central subject in various disciplines to reveal the links between swarming behaviors and individual interaction laws.

A common belief in scientific research is that complicated swarming behaviors are the consequences of simple interactions, for instance, the interactions depending on pairwise distances.

*Department of Applied Mathematics and Statistics, Johns Hopkins University. Email: jfeng34@jhu.edu
†Department of Mathematics, University of California Santa Barbara. Email: charles@math.ucsb.edu
‡Department of Mathematics, and Physics, Harvard University. Email: yren@g.harvard.edu
§Department of Mathematics, University of California Santa Barbara. Email: suitang@ucsb.edu

Inspired by physics, one can write down a second-order ODE system for N interacting particles $\boldsymbol{x}_1, \cdots, \boldsymbol{x}_N$ in $\mathbb{R}^d$ as follows: for $i = 1, \cdots, N$, the i-th equation for $\boldsymbol{x}_i$ is

$$m_i \ddot{\boldsymbol{x}}_i(t) = F_i(\boldsymbol{x}_i(t), \dot{\boldsymbol{x}}_i(t), \boldsymbol{\alpha}_i) + \underbrace{\sum_{i'=1}^{N} \frac{1}{N} \Big[\phi(\|\boldsymbol{x}_{i'}(t) - \boldsymbol{x}_i(t)\|)(\boldsymbol{x}_{i'}(t) - \boldsymbol{x}_i(t)) \Big]}_{\text{interaction force}}. \tag{1}$$

The form of the above governing equation is derived from Newton's second law: m_i is the mass of the agent i; $\ddot{\boldsymbol{x}}_i$ is the acceleration; $\dot{\boldsymbol{x}}_i$ is the velocity; F_i is a parametric function of the position and velocity, modeling frictions of the particles with the environment; the scalar parameters $\boldsymbol{\alpha}_i$ describe the friction strength; and the interaction force is the i-th component of the derivative of a potential energy function $\mathcal{U}$ depending on pairwise distances:

$$\mathcal{U}(\boldsymbol{X}(t)) := \sum_{i,i'=1}^{N} \frac{1}{2N} \Phi(\|\boldsymbol{x}_{i'}(t) - \boldsymbol{x}_i(t)\|), \Phi'(r) = \phi(r) r, \tag{2}$$

where $\|\cdot\|$ is the Euclidean norm and ϕ is the interaction kernel function $\phi : \mathbb{R}^+ \to \mathbb{R}$.

There are remarkable achievements in the qualitative study of the system (1) and its variants. Despite the simple form of the interactions, the asymptotic behavior of the solutions to (1) has proven to reproduce a wide variety of macroscopic collective patterns (D'Orsogna et al., 2006; Motsch and Tadmor, 2014; Baumann et al., 2020; Chuang et al., 2007) which are similar to those observed in practice. System (1) and its variants also find various applications in optimization (Mei et al., 2018) and sampling (Liu, 2017) in machine learning. Despite the impressive progress, the governing interacting potentials and parametric form of friction force are still far from being *precisely* determined for many systems that arise in biology, ecology, and social science.

The recent rapid advancements in digital imaging and high-resolution lightweight GPS devices have made the trajectory data of interacting particle systems increasingly available. This motivated us to consider the fundamental inverse problem: given the trajectory data generated from (1), can we discover the governing equation? Furthermore, what are effective algorithms with theoretical guarantees? There are several challenges we face. The first one is non-linearity. The friction force often depends *nonlinearly* with respect to the scalar parameters $\boldsymbol{\alpha}$. Thus, solving the inverse problem involves nontrivial separations between the friction force and interaction force constrained to dynamics. The second challenge results from little information on the analytic forms of interaction kernels. For example, the Morse type kernels and Lennard-Jones type kernels have very different parametric forms, but they are well-known to reproduce similar collective patterns in particle dynamics. Ideally, we want to make *minimal* assumptions on their analytic forms and infer them in a nonparametric fashion. This involves working with large and flexible infinite-dimensional function spaces (e.g, Sobolev spaces). Thirdly, in practical scenarios, it is possible that only a small amount of data is available, i.e., M, L is small, and the data may have some stochastic effects such as noises. In such scenarios, obtaining quantitative predictive uncertainties in estimated interaction kernels is crucial for quantifying the reliability of estimators. This information is useful in designing a data acquisition plan, known as active learning (Cohn et al., 1996), which can be used to optimally enhance our knowledge about the system. In summary, we seek an algorithm that can simultaneously perform inference of $\boldsymbol{\alpha}$, which incorporates the parametric form of $\boldsymbol{F}$, and nonparametric inference of ϕ while also providing uncertainty quantification of the learned models.

In machine learning, Gaussian process (GP) based approaches have well-documented merits not only in superior learning of a rich class of nonlinear functions without assumptions on

their parametric form in the scarce noisy data regime, but also in quantifying the associated uncertainty. This makes a GP based approach attractive for our learning problem. We propose a novel approach by modeling ϕ as Gaussian processes and incorporating the GPs into the structure of the whole ODE system (1). The probabilistic framework brought by GPs enables us to perform joint parametric inference of $\boldsymbol{\alpha}$ and nonparametric inference of ϕ via the powerful model selection procedure of GPs. The resulting algorithm has superior performance in the scarce noisy data regime and yields estimators with uncertainty quantification. We shall show that it is computationally efficient, statistically sound, and effective in benchmark systems.

1.1 Summary/overview of the proposed algorithm

First-order systems For demonstration purposes, we first summarize the key ideas of the GP based algorithm for the first order system: for $i = 1, \cdots, N$, one has

$$\dot{\boldsymbol{x}}_i(t) = \frac{1}{N} \sum_{i'=1}^{N} \phi\left(\|\boldsymbol{x}_{i'}(t) - \boldsymbol{x}_i(t)\|\right)(\boldsymbol{x}_{i'}(t) - \boldsymbol{x}_i(t)), \tag{3}$$

where $\boldsymbol{x}_i(t), \dot{\boldsymbol{x}}_i(t) \in \mathbb{R}^d$ are the position and velocity of i-th agent at time t; $\phi : \mathbb{R}^+ \to \mathbb{R}$ governs the pairwise interactions. Our observations consist of $\{\boldsymbol{x}_i^{(m)}(t_l), \dot{\boldsymbol{x}}_i^{(m)}(t_l) + \boldsymbol{\epsilon}_i^{(m,l)}\}_{i,m,l=1}^{N,M,L}$, with L time instances $0 = t_1 < t_2 \cdots < t_L = T$; M being the number of trajectories, and the initial positions $\{\boldsymbol{x}_i^{(m)}(0) : 1 \le i \le N\}$ are drawn i.i.d from an unknown probability measure μ_0 defined on the state space $\mathbb{R}^{dN}$; the Gaussian noise $\boldsymbol{\epsilon}_i^{(m,l)} \overset{i.i.d}{\sim} \mathcal{N}(\mathbf{0}, \sigma^2 I_{d\times d})$ is independent of μ_0. The noise model we adapt here can be viewed as a discretization of corresponding Stochastic Differential Equations (SDEs) with homogeneous Brownian noise and is used to model the random effects of the environment on the measurement of velocities or imposing frictions. We shall see immediately that the Gaussian noise term serves the role of regularization in the proposed GP framework (see (8) below). In this paper, we are interested in the data regime where L is fixed and M varies. That is to say, we observe data coming from multiple independent trajectories of fixed length.

For ease of presentation, we use a compact notation to represent the ODEs (3)

$$\dot{\boldsymbol{X}}(t) = \mathbf{f}_\phi(\boldsymbol{X}(t)), \tag{4}$$

where $\boldsymbol{X} = [\boldsymbol{x}_1^\top, \cdots, \boldsymbol{x}_N^\top]^\top \in \mathbb{R}^{dN}$ denotes the full state vector, and $\mathbf{f}_\phi : \mathbb{R}^{dN} \to \mathbb{R}^{dN}$ represents the distance based interactions governed by the interaction kernel ϕ as in (1). We use the notation $\mathbb{Y}_{\sigma^2,M} = \{\mathbb{X}_M, \mathbb{V}_{\sigma^2,M}\}$ to denote the noisy observed trajectory data, where we introduce two vectors

$$\mathbb{X}_M = \mathrm{Vec}\big(\{\boldsymbol{X}^{(m)}(t_l)\}_{m,l=1}^{M,L}\big) \in \mathbb{R}^{dNML} \tag{5}$$

$$\mathbb{V}_{\sigma^2,M} = \mathrm{Vec}\big(\{\dot{\boldsymbol{X}}^{(m)}(t_l) + \boldsymbol{\epsilon}^{(m,l)}\}_{m,l=1}^{M,L}\big) \in \mathbb{R}^{dNML}. \tag{6}$$

Our proposed algorithm consists of three steps. We start by modeling ϕ as a Gaussian process (Williams and Rasmussen, 2006), i.e., consider the prior $\phi \sim \mathcal{GP}(0, K_\theta(r, r'))$, with mean zero and covariance kernel function K_θ which depends on hyper-parameters θ. This prior incorporates our prior knowledge about the underlying interaction rule. Secondly, we leverage the powerful training procedure of GP to choose a data-driven prior, i.e., updating θ by maximizing the likelihood of the observational data. That is equivalent to minimizing the negative log-likelihood function

$$\mathrm{argmin}_{\theta,\sigma^2} - \log \mathbb{P}(\mathbb{V}_{\sigma^2,M} | \mathbb{X}_M, \theta, \sigma^2), \tag{7}$$

where we estimate the noise level (σ^2) of our observations at the same time. In our setting, $\mathbf{f}_\phi$ is linear in ϕ, i.e., $\mathbf{f}_{\phi_1+\phi_2} = \mathbf{f}_{\phi_1} + \mathbf{f}_{\phi_2}$, and observational noises are Gaussians which are independent of trajectory data. Therefore, $\mathbb{P}(\mathbb{V}_{\sigma^2,M}|\mathbb{X}_M, \theta)$ is still Gaussian. One can write its explicit formula and its gradients with respect to hyper-parameters. This allows us to use an efficient variant of the conjugate gradient method to find a minimizer $\hat{\theta}$. We now denote $\widehat{K} = K_{\hat{\theta}}$.

Finally, we use the posterior mean estimator to predict the value of ϕ at a testing location $r^* \in \mathbb{R}^+$. Leveraging the fact that the joint distribution of $\mathbf{f}_\phi$ and ϕ according to the prior is still Gaussian, we use a conditioning argument to obtain the following closed-form formula

$$\bar{\phi}_M(r^*) = \widehat{K}_{\phi,\mathbf{f}_\phi}(r^*, \mathbb{X}_M)(\widehat{K}_{\mathbf{f}_\phi}(\mathbb{X}_M, \mathbb{X}_M) + \sigma^2 I)^{-1}\mathbb{V}_{\sigma^2,M}, \tag{8}$$

where the matrices $\widehat{K}_{\phi,\mathbf{f}_\phi}(r^*, \mathbb{X}_M) \in \mathbb{R}^{1\times dNML}$ and $\widehat{K}_{\mathbf{f}_\phi}(\mathbb{X}_M, \mathbb{X}_M) \in \mathbb{R}^{dNML\times dNML}$ denote the covariance matrix between $\phi(r^*)$ and $\mathbf{f}_\phi(\mathbb{X}_M)$, and $\mathbf{f}_\phi(\mathbb{X}_M)$ and $\mathbf{f}_\phi(\mathbb{X}_M)$ respectively; I is the identity matrix of compatible size. In addition, we can also quantify the uncertainty of estimation at r^* by

$$\mathrm{Var}(\bar{\phi}_M|\mathbb{Y}_{\sigma^2,M}) = \widehat{K}(r^*, r^*) - \widehat{K}_{\phi,\mathbf{f}_\phi}(r^*, \mathbb{X}_M)(\widehat{K}_{\mathbf{f}_\phi}(\mathbb{X}_M, \mathbb{X}_M) + \sigma^2 I)^{-1}\widehat{K}_{\mathbf{f}_\phi,\phi}(\mathbb{X}_M, r^*), \tag{9}$$

where $\widehat{K}_{\mathbf{f}_\phi,\phi}(\mathbb{X}_M, r^*) \in \mathbb{R}^{dNML\times 1}$ is the transpose of $\widehat{K}_{\phi,\mathbf{f}_\phi}(r^*, \mathbb{X}_M)$ (See Corollary 6 for the derivation).

Extension to systems with external forces and second-order systems The proposed approach can be easily generalized to the variants. For example, consider the first-order system with unknown external forces

$$\dot{\boldsymbol{X}}(t) = \mathbf{f}_\phi(\boldsymbol{X}(t)) + \boldsymbol{F}(\boldsymbol{X}(t), \boldsymbol{\alpha}), \tag{10}$$

where $\boldsymbol{F}(\boldsymbol{X}(t), \boldsymbol{\alpha}) : \mathbb{R}^{dN} \to \mathbb{R}^{dN}$ is a parametric function of *unknown* scalar parameters $\boldsymbol{\alpha}$ ($\boldsymbol{F}$ can depend nonlinearly on $\boldsymbol{\alpha}$). The parametric form of $\boldsymbol{F}$ encodes the physical constraints of the underlying system. In this case, we can treat both $\boldsymbol{\alpha}$ and σ^2 (the noise level) as hyper-parameters and solve

$$\mathrm{argmin}_{\theta,\boldsymbol{\alpha},\sigma^2} - \log \mathbb{P}(\mathbb{V}_{\sigma^2,M}|\mathbb{X}_M, \theta, \boldsymbol{\alpha}, \sigma^2).$$

Even though the above optimization is in general non-convex, our numerical examples show that one can find accurate estimations of $\boldsymbol{\alpha}$ and σ^2 (the noise level) using a few iterations (≈ 50) from a small set of training data. Finally, we plug these estimates into the model and perform the prediction of ϕ using a posterior mean similar to (8). In section 2, we provide full technical details of the proposed approach to general second-order systems with unknown external forces.

1.2 Literature review and the novelty of our work

Many recent works have applied machine learning tools to the discovery of dynamical systems, leading to the formulation of new general principles. The resulting methods can be divided into two main categories: (1) methods based on variants of deep neural networks (DNNs) (Long et al., 2018; Raissi, 2018; Raissi et al., 2018; Qin et al., 2019; Li et al., 2021; Wang et al., 2021); and (2) methods based on kernel methods and Gaussian processes (Archambeau et al., 2007; Raissi et al., 2017; Heinonen et al., 2018; Yildiz et al., 2018; Mao et al., 2019; Zhao et al., 2020; Chen et al., 2020; Lee et al., 2020; Yang et al., 2021; Wang and Zhou, 2021; Chen et al., 2021; Stepaniants, 2021). However, methods of type (2) have the potential for considerable advantages over those of type (1), both in terms of theoretical analysis and numerical implementation (Chen et al., 2021). In a nutshell, there is no single method that works best in all settings and the theoretical

results are still scarce. It is necessary and requires nontrivial effort to propose and develop a theoretical understanding of learning methodology for a particular type of dynamical system and data regime, as one has to face the unique challenges caused by the underlying physical constraints and the observational data.

In this paper, we cast the data estimation problem arising in the particle swarm models (1) as a statistical inverse learning problem and develop a simple and rigorous kernel/Gaussian process framework for solving it. Below we shall compare our work with the works using Gaussian processes and existing works for particle swarm models.

Novelty of the algorithm Our method is different from other GP based approaches introduced to learn ODEs from observations: they either model $\mathbf{f}_\phi : \mathbb{R}^{dN} \to \mathbb{R}^{dN}$ as a GP, ignoring the interacting structure, and solve a regression problem which would be cursed by the high dimension of the state space of $\boldsymbol{X}$, e.g.(Heinonen et al., 2018), or assume independent GP prior distributions on each component of $\boldsymbol{X}$, and consider learning a parametric function (Mao et al., 2019; Yang et al., 2021). We instead model the latent function ϕ as a GP and solve an inverse problem by restricting the GP on a manifold that satisfies the ODE system. In this way, we offer a nonparametric approach, with minimal assumptions on ϕ, and build the invariance of the equations under permutation of the agents as well as the radial symmetry of ϕ into the machine learning model of $\mathbf{f}_\phi$, and therefore avoid the curse of dimensionality. The methodology we introduce has the following properties:

- theoretically, the proposed method is amenable to rigorous analysis. We establish a novel operator-theoretical framework, suggesting new research directions to generalize the analysis of kernel regression methods (Williams and Rasmussen, 2006) and linear inverse problems to interacting particle systems. Under Hölder type source conditions on ϕ, we prove the reconstruction error converges at an upper rate in M (see Theorem 25):

$$\|\bar{\phi}_M - \phi\|_{\mathcal{H}_K} \lesssim M^{\frac{-\gamma}{2\gamma+2}}$$

  where $\mathcal{H}_K$ is the underlying Reproducing Kernel Hilbert Space (RKHS) and $0 < \gamma \leq \frac{1}{2}$. Based on our best knowledge, there is no prior published work on the application of GP to particle swarm models (1) in this way and our paper is the first one to obtain the theoretical convergence rates in an RKHS norm. We remark this upper rate in M is statistically optimal for target functions satisfying certain source conditions and can not be further improved. One can refer to (Blanchard and Mücke, 2018) which established the minimax rates for classical linear statistical inverse problems; our case corresponds to $s = 0$ (reconstruction error) and $b \to 1^+$ (as we deal with all Mercer kernels) in their main result. Using our framework as the bridge, we believe one can obtain more refined rates and bounds in the future. As a byproduct, we also show that a parametric rate in M for the L^∞ norm of the marginal posterior variance can be obtained, and furthermore, this rate could also involve the number of particles and the number of observational time instances (see Theorem 26). Last but not least, the reconstruction error bound also yields bounds on trajectory predictions even if our observation data is *finite* and obtained from discrete time instances. Let $\hat{\boldsymbol{X}}_{[0,T]}$ denote the trajectory generated by the estimator $\hat{\phi}$ over the time interval $[0, T]$, given the same initial condition, then application of Grönwall's inequality (Ames and Pachpatte, 1997) implies

$$\|\hat{\boldsymbol{X}}_{[0,T]} - \boldsymbol{X}_{[0,T]}\| \lesssim \|\hat{\phi} - \phi\|_{\mathcal{H}_K}.$$

  Such a trajectory prediction error bound is only available in previous works (Lu et al., 2019, 2020, 2021; Miller et al., 2020) where one has continuous-time observational data. This demonstrates the benefit of using stronger RKHS norms.

- computationally, it inherits the complexity of state-of-the-art solvers for kernel matrices, suggesting new research directions to generalize the work of optimal approximate methods for linear regression (Quinonero-Candela and Rasmussen, 2005; Schäfer et al., 2021), to the proposed setting of solving parameter and kernel identification in particle swarm models. See more discussions in section 3.7.

The existing works on the data-driven discovery of interacting particle systems Motivated by the broad applications of interacting particle systems in various disciplines, the data-driven discovery of interacting particle systems has become a highly active area of research in recent years. We will first briefly review the relevant works on stochastic interacting particle systems. The most frequently studied approach in recent works is the maximum likelihood approach, which includes parameter estimation (Kasonga, 1990; Bishwal et al., 2011; Gomes et al., 2019; Chen, 2021; Sharrock et al., 2021) and nonparametric estimation of drift in the stochastic McKean-Vlasov equation (Genon-Catalot and Larédo, 2022; Della Maestra and Hoffmann, 2022; Yao et al., 2022), as well as radial interaction kernel learning in (Lu et al., 2021). One can also refer to (Messenger and Bortz, 2021) for the development of the Weak SINDy algorithm that leverages the weak form of the differential equation and sparse parametric regression, with applications to cellular dynamics (Messenger et al., 2022).

Our work is on the non-parametric methods for deterministic microscopic interacting particle systems. The theoretical study of the least square approach for learning ϕ in first-order systems was proposed in (Bongini et al., 2017). Later, it has been generalized to second-order systems and heterogeneous systems in (Lu et al., 2019), with theoretical developments in (Lu et al., 2020, 2021; Miller et al., 2020). Compared with previous work that only focused on learning interaction kernels, our proposed method has the following advantages: (1) it can handle more difficult yet more practical scenarios, i.e., joint inference of scalar parameters $\boldsymbol{\alpha}$ and ϕ, as both are often unknown in practical scenarios. Therefore, our method can learn the governing equations (1). (2) It provides uncertainty quantification on estimators. In the ideal data regime, we provide a rigorous analysis and show how it depends on the system parameters. This uncertainty measures the reliability of our estimators, in particular, it can be used to measure the mismatch between our proposed models with the real-world systems. (3) It has a powerful training procedure to select a data-driven prior and this overcomes the drawback of the previous least square algorithms: there is no criterion to select the optimal choice of function spaces (in terms of both basis and dimensions) for learning so as to minimize the generalization error. We show in Example 4.2 that this yields better performance in trajectory predictions with unseen datasets.

The theories developed in this paper are related to but significantly depart from previous work on studying least square estimators (Lu et al., 2019, 2020, 2021; Miller et al., 2020). We shall show the posterior mean estimators can be viewed as KRR estimators, whose risk functionals are the *regularized* version of those proposed in previous works by setting the underlying hypothesis space to be an appropriate RKHS space. We go much further beyond the existing analysis:

- Our new and rigorous operator-theoretic framework formulates this learning problem as a linear statistical inverse problem. This allows us to refine the analysis for target functions under source conditions and obtain convergence in the *stronger* Reproducing Kernel Hilbert Space (RKHS) norm. From the perspective of the inverse problem, we analyze the reconstruction error while the previous works analyzed the residual error, where only L^2 error bounds were obtained. We remark that the analysis framework presented in (Lu et al., 2019, 2020) can not be extended directly to the RKHS norm and our operator-theoretical framework is significantly different than the previous ones.

- We study noisy trajectory data and provide error bounds on uncertainties that noise brings

to the estimation, while the previous works only dealt with noise-free trajectory data.

To summarize, our contribution can be briefly stated as

- A novel GP-based algorithm that can solve joint parametric and nonparametric inference in the particle swarm model.
- Rigorous analysis on recoverability, quantitative error bounds, and establishing the statistical optimality of both posterior mean and variance estimators in the framework of linear statistical inverse problems.
- Extensive numerical experiments demonstrating the effectiveness and advantages over previous approaches.

1.3 Outline and organization of the paper

Our paper is organized as follows: in section 2, we present the algorithm for second-order systems of form (1). In section 3, we establish a novel operator-theoretic framework to analyze the performance of the posterior mean estimators and marginal posterior variance. Finally, we test the effectiveness and demonstrate the advantages of the proposed approach on several benchmark systems exhibiting different types of swarming behaviour.

1.4 Notation and preliminaries

Notation Let ρ be a Borel positive measure on D dimensional Eucliean space $\mathbb{R}^D$. We use $L^2(\mathbb{R}^D;\rho;\mathbb{R}^n)$ to denote the set of $L^2(\rho)$-integrable vector-valued functions that map $\mathbb{R}^D$ to $\mathbb{R}^n$. For a function $\boldsymbol{f} \in L^2(\mathbb{R}^D;\rho;\mathbb{R}^n)$, and a vector $\boldsymbol{X} = [\boldsymbol{x}_1^\top, \cdots, \boldsymbol{x}_m^\top]^T \in \mathbb{R}^{mD}$ with $\boldsymbol{x}_i \in \mathbb{R}^D$, we use the notation $\boldsymbol{f}(\boldsymbol{X})$ to represent the image of the vector under the function of $\boldsymbol{f}$ componentwisely, namely, $\boldsymbol{f}(\boldsymbol{X}) = [\boldsymbol{f}(\boldsymbol{x}_1)^\top, \cdots, \boldsymbol{f}(\boldsymbol{x}_m)^\top]^\top \in \mathbb{R}^{mn}$. Let $\mathcal{S}_1$ be a measurable subset of $\mathbb{R}^m$, then the restriction of the measure ρ on $\mathcal{S}_1$, denoted by $\rho \llcorner \mathcal{S}_1$, is defined as $\rho \llcorner \mathcal{S}_1(\mathcal{S}_2) = \rho(\mathcal{S}_1 \cap \mathcal{S}_2)$ for any measurable subset $\mathcal{S}_2$ of $\mathbb{R}^D$. We used $\mathcal{N}(0, I_{d\times d})$ to denote the standard multivariate Gaussian distribution in $\mathbb{R}^d$.

Preliminaries on GPs (Gaussian Processes) Prior We say $\phi \sim \mathcal{GP}(u, K)$ to denote our prior on ϕ. In particular, this means that for any $r \in \mathbb{R}$, the random variable $\phi(r)$ is Gaussian: $\phi(r) \sim \mathcal{N}(u(r), K(r,r))$, where $\mathcal{N}$ denotes the normal or multivariable normal distributions. Similarly, the joint distribution of $\begin{bmatrix}\phi(r)\\ \phi(r')\end{bmatrix}$ is multivariate Gaussian: $\begin{bmatrix}\phi(r)\\ \phi(r')\end{bmatrix} \sim \mathcal{N}\left(\begin{bmatrix}(u(r)\\ (u(r')\end{bmatrix}, \begin{bmatrix}K(r,r) & K(r,r')\\ K(r',r) & K(r',r')\end{bmatrix}\right)$. This extends in a natural way to any finite set $(r_1, \ldots, r_N) \in \mathbb{R}^N$.

Preliminaries on operator algebras Let $\mathcal{H}_1, \mathcal{H}_2$ be Hilbert spaces. We use $\langle\cdot,\cdot\rangle_{\mathcal{H}_1}$ to denote the inner product over $\mathcal{H}_1$, and still use $\langle\cdot,\cdot\rangle$ to denote the inner product on the Euclidean space. We denote by $\mathcal{B}(\mathcal{H}_1, \mathcal{H}_2)$ the set of bounded linear operators mapping $\mathcal{H}_1$ to $\mathcal{H}_2$. Let $A \in \mathcal{B}(\mathcal{H}_1, \mathcal{H}_2)$, we use $\mathrm{Im}(A)$ to denote its range and $\|A\|$ to denote its operator norm. A is a compact operator if A maps bounded subsets of $\mathcal{H}_1$ to relatively compact subsets of $\mathcal{H}_2$ (subsets with compact closure in $\mathcal{H}_2$). We use $A^* : \mathcal{H}_2 \to \mathcal{H}_1$ to denote the adjoint operator of A, that is, $\forall f \in \mathcal{H}_1$, $g \in \mathcal{H}_2$, $\langle Af, g\rangle_{\mathcal{H}_2} = \langle f, A^*g\rangle_{\mathcal{H}_1}$. $A \in \mathcal{B}(\mathcal{H}_1, \mathcal{H}_1)$ is said to be positive if $A^* = A$ and $\langle Ah, h\rangle_{\mathcal{H}_1} \geq 0$ for all $h \in \mathcal{H}_1$. If A is a real-valued matrix, $A^* = A^\top$, the transpose of the matrix.

If $A \in \mathcal{B}(\mathcal{H}_1, \mathcal{H}_1)$ is a compact positive operator, and λ_n represents the n-th eigenvalue in decreasing order, then, by the spectral theory of compact operators, the eigenfunctions $\{\varphi_n\}_{n=1}^N$ (possibly with $N = \infty$) of A form an orthonormal basis for $\mathcal{H}_1$ so that $A^\tau \psi = \sum_{n=1}^N \lambda_n^\tau \langle \varphi_n, \psi \rangle_{\mathcal{H}_1} \varphi_n$ for a real number τ. If $\tau < 0$, the domain of A^τ is on the subspace S_τ of $\mathcal{H}_1$ given by $S_\tau = \{\sum_{n=1}^N a_n \varphi_n | \sum_{n=1}^N (a_n \lambda_n^\tau)^2 \text{ is convergent}\}$. If $h \notin S_\tau$, then $\|A^\tau h\|_{\mathcal{H}_1} = \infty$.

Let $\mathcal{H}$ be a Hilbert space, and $A, B \in \mathcal{B}(\mathcal{H}, \mathcal{H})$. For two self-adjoint operators A, B, that is, $A^* = A$ and $B^* = B$, we say that $A \geq B$ if $A - B$ is a positive operator, i.e. $\langle (A-B)h, h \rangle_{\mathcal{H}} \geq 0$ for all $h \in \mathcal{H}$. Let $\{e_i\}_{i \in I}$ be an orthonormal basis of $\mathcal{H}$. The trace of B is defined as $\mathrm{Tr}(B) = \sum_{i \in I} \langle Be_i, e_i \rangle_{\mathcal{H}}$. A is a Hilbert Schmidt operator if $\sum_{i \in I} \|Ae_i\|_{\mathcal{H}}^2 < \infty$, i.e., $\mathrm{Tr}(A^*A) < \infty$. $\|A\|_{HS}$ denotes its Hilbert–Schmidt norm that satisfies $\|A\|_{HS}^2 = \mathrm{Tr}(A^*A)$. A is said to be in the trace class if $\mathrm{Tr}(|A|) < \infty$ for $|A| = \sqrt{A^*A}$. Hilbert Schmidt operators and trace class operators are compact.

For $d, N, M, L \in \mathbb{N}^+$, let $\boldsymbol{w} = (\boldsymbol{w}_{m,l,i})_{m,l,i=1}^{M,L,N}, \boldsymbol{z} = (\boldsymbol{z}_{m,l,i})_{m,l,i=1}^{M,L,N} \in \mathbb{R}^{dNML}$ with $\boldsymbol{w}_{m,l,i}, \boldsymbol{z}_{m,l,i} \in \mathbb{R}^d$, we define

$$\langle \boldsymbol{w}, \boldsymbol{z} \rangle = \frac{1}{MLN} \sum_{m,l,i=1}^{M,L,N} \langle \boldsymbol{w}_{m,l,i}, \boldsymbol{z}_{m,l,i} \rangle, \tag{11}$$

where $\langle \boldsymbol{w}_{m,l,i}, \boldsymbol{z}_{m,l,i} \rangle$ is the canonical inner product on $\mathbb{R}^d$ (without normalization).

Preliminaries on RKHSs Let $\mathcal{D}$ be a compact subset of $\mathbb{R}^D$. We say that $K : \mathcal{D} \times \mathcal{D} \to \mathbb{R}$ is a Mercer Kernel if it is continuous, symmetric, and positive semidefinite, i.e., for any finite set of distinct points $\{x_1, \cdots, x_M\} \subset \mathcal{D}$, the matrix $(K(x_i, x_j))_{i,j=1}^M$ is positive semidefinite. For $x \in \mathbb{R}^D$, K_x is a function defined on $\mathcal{D}$ such that $K_x(y) = K(x, y)$, $y \in \mathcal{D}$. The Moore–Aronszajn theorem proves that there is an RKHS $\mathcal{H}_K$ associated with the kernel K, which is defined to be the closure of the linear span of the set of functions $\{K_x : x \in \mathcal{D}\}$ with respect to the inner product $\langle \cdot, \cdot \rangle_{\mathcal{H}_K}$ satisfying $\langle K_x, K_y \rangle_{\mathcal{H}_K} = K(x, y)$.

To ensure the system (1) has a unique solution for arbitrary initial conditions, we assume the true interaction kernel ϕ_{true} lies in a suitable function space.

Assumption 1. *ϕ_{true} lies in a RKHS $\mathcal{H}_K$ spanned by a Mercer Kernel K defined on $[0, R] \times [0, R]$ for some $R > 0$. In particular, $\kappa^2 = \sup_{r \in [0,R]} K(r, r) < \infty$.*

Assumption 1 implies that functions in $\mathcal{H}_K$ are continuous. Examples of RKHSs include common Sobolev spaces used in the differential equation literature. It is important to note that we only use this assumption in our theoretical analysis. In our numerical section, we use the Matérn kernel, and our interaction function is not necessarily compactly supported.

For the sake of conciseness, we will drop the subscript and use ϕ to represent the true interaction kernel.

2 GP Based algorithm for second-order systems with external forces

In this section, we present the algorithm for the second-order particle swarm model: for $i = 1, \cdots, N$,

$$m_i \ddot{\boldsymbol{x}}_i(t) = \boldsymbol{F}_i(\boldsymbol{x}_i(t), \dot{\boldsymbol{x}}_i(t), \boldsymbol{\alpha}_i) + \sum_{i'=1}^N \frac{1}{N} \Big[\phi(\|\boldsymbol{x}_{i'}(t) - \boldsymbol{x}_i(t)\|)(\boldsymbol{x}_{i'}(t) - \boldsymbol{x}_i(t)) \Big]. \tag{12}$$

We shall use the compact form of a second-order system as follows

$$\boldsymbol{Z}(t) = \boldsymbol{F}(\boldsymbol{Y}(t), \boldsymbol{\alpha}) + \mathbf{f}_\phi(\boldsymbol{X}(t)). \tag{13}$$

We summarize the notation in Table 1.

Table 1: Notation for second-order systems

Variable	Definition
$\boldsymbol{X} \in \mathbb{R}^{dN}$	vectorization of position vectors $(\boldsymbol{x}_i)_{i=1}^N$
$\boldsymbol{V} \in \mathbb{R}^{dN}$	vectorization of velocity vectors $(\boldsymbol{v}_i)_{i=1}^N = (\dot{\boldsymbol{x}}_i)_{i=1}^N$
$\boldsymbol{Y} \in \mathbb{R}^{2dN}$	$\boldsymbol{Y} = (\boldsymbol{X}, \boldsymbol{V})^T$
$\boldsymbol{Z} \in \mathbb{R}^{dN}$	vectorization of $(m_i \ddot{\boldsymbol{x}}_i)_{i=1}^N$
$\boldsymbol{r}_{ij}^{\boldsymbol{X}}, \boldsymbol{r}_{ij}^{\boldsymbol{X}'} \in \mathbb{R}^d$	$\boldsymbol{x}_j - \boldsymbol{x}_i$, $\boldsymbol{x}_j' - \boldsymbol{x}_i'$
$r_{ij}^{\boldsymbol{X}}, r_{ij}^{\boldsymbol{X}'} \in \mathbb{R}^+$	$r_{ij}^{\boldsymbol{X}} = \|\boldsymbol{r}_{ij}^{\boldsymbol{X}}\|, r_{ij}^{\boldsymbol{X}'} = \|\boldsymbol{r}_{ij}^{\boldsymbol{X}'}\|$
$\boldsymbol{F}(\cdot, \boldsymbol{\alpha})$	the non-collective force with parameter $\boldsymbol{\alpha}$
$\mathbf{f}_\phi$	energy-based interaction force field
$\mathrm{vec}(\{a_i\}_{i=1}^n) \in \mathbb{R}^n$	$\mathrm{vec}(\{a_i\}_{i=1}^n) = (a_1, \ldots, a_n)^T$, vectorization of the set $\{a_i\}_{i=1}^n$

Note that if $m_i = 0$ for all i, then the system (12) becomes a first-order system. We are interested in learning ϕ and $\boldsymbol{\alpha}$ from data. By modeling ϕ as a GP, the joint distribution of the acceleration field at any two time instances is still Gaussian, as shown in the following lemma:

Lemma 2. *Let ϕ be a Gaussian process with mean zero and covariance function $K_\theta : [0, R] \times [0, R] \to \mathbb{R}$, i.e., $\phi \sim \mathcal{GP}(0, K_\theta(r, r'))$, and $\boldsymbol{Z}(t) = \boldsymbol{F}(\boldsymbol{Y}(t), \boldsymbol{\alpha}) + \mathbf{f}_\phi(\boldsymbol{X}(t))$ as defined in (13). Then for any $t, t' \in [0, T]$, we have that,*

$$\begin{bmatrix} \boldsymbol{Z}(t) \\ \boldsymbol{Z}(t') \end{bmatrix} \sim \mathcal{N}\left(\begin{bmatrix} \boldsymbol{F}(\boldsymbol{Y}(t), \boldsymbol{\alpha}) \\ \boldsymbol{F}(\boldsymbol{Y}(t'), \boldsymbol{\alpha}) \end{bmatrix}, K_{\mathbf{f}_\phi}(\boldsymbol{X}(t), \boldsymbol{X}(t')) \right), \tag{14}$$

where $K_{\mathbf{f}_\phi}(\boldsymbol{X}(t), \boldsymbol{X}(t')))$ is the covariance matrix $\mathrm{Cov}(\mathbf{f}_\phi(\boldsymbol{X}(t)), \mathbf{f}_\phi(\boldsymbol{X}(t')))$ with the (i, j)-th block

$$\mathrm{Cov}([\mathbf{f}_\phi(\boldsymbol{X})]_i, [\mathbf{f}_\phi(\boldsymbol{X}')]_j) = \frac{1}{N^2} \sum_{k \neq i, k' \neq j} K_\theta(r_{ik}^{\boldsymbol{X}}, r_{jk'}^{\boldsymbol{X}'}) \boldsymbol{r}_{ik}^{\boldsymbol{X}} \boldsymbol{r}_{jk'}^{\boldsymbol{X}'^T}. \tag{15}$$

Proof. Since $\phi \sim \mathcal{GP}(0, K_\theta(r, r'))$, for any $r, r' \in [0, R]$, we have that,

$$\mathbb{E}[\phi(r)] = 0, \tag{16}$$
$$\mathrm{Cov}[\phi(r), \phi(r')] = K_\theta(r, r'). \tag{17}$$

Therefore, for any collection of states $\{r_i\}_{i=1}^n \subset [0, R]$, and $\{a_i\}_{i=1}^n, \{b_i\}_{i=1}^n \subset \mathbb{R}$, the linear operator on function values $\mathcal{L}(\{\phi(r_i)\}_{i=1}^n) := (a_i \phi(r_i) + b_i)_{i=1}^n$ satisfies

$$\mathcal{L}(\{\phi(r_i)\}_{i=1}^n) \sim \mathcal{N}(\mathrm{vec}(\{b_i\}_{i=1}^n), \Sigma_{\mathcal{L}(\phi)}), \tag{18}$$

where $\mathcal{N}$ denotes the Gaussian distribution, $\mathrm{vec}(\{b_i\}_{i=1}^n) \in \mathbb{R}^n$ is the vectorization of $\{b_i\}_{i=1}^n$, and the covariance matrix $\Sigma_{\mathcal{L}(\phi)} = \{a_i a_j K_\theta(r_i, r_j)\}_{i,j=1}^n \in \mathbb{R}^{n \times n}$.

Note that

$$[\mathbf{f}_\phi(\boldsymbol{X}(t))]_i = \sum_{i'=1}^N \frac{1}{N} \phi(\|\boldsymbol{x}_{i'} - \boldsymbol{x}_i\|)(\boldsymbol{x}_{i'} - \boldsymbol{x}_i), \tag{19}$$

which is linear in ϕ. So for any t, t', using (18), we have that,

$$\begin{bmatrix}\mathbf{f}_\phi(\boldsymbol{X}(t))\\ \mathbf{f}_\phi(\boldsymbol{X}(t'))\end{bmatrix} \sim \mathcal{N}(\mathbf{0}, K_{\mathbf{f}_\phi}(\boldsymbol{X}(t), \boldsymbol{X}(t'))), \tag{20}$$

where $K_{\mathbf{f}_\phi}(\boldsymbol{X}(t), \boldsymbol{X}(t')))$ is the covariance matrix $\mathrm{Cov}(\mathbf{f}_\phi(\boldsymbol{X}(t)), \mathbf{f}_\phi(\boldsymbol{X}(t')))$ with the (i,j)-th block

$$\mathrm{Cov}([\mathbf{f}_\phi(\boldsymbol{X})]_i, [\mathbf{f}_\phi(\boldsymbol{X}')]_j) = \frac{1}{N^2}\sum_{k\neq i, k'\neq j} K_\theta(r_{ik}^{\boldsymbol{X}}, r_{jk'}^{\boldsymbol{X}'})\boldsymbol{r}_{ik}^{\boldsymbol{X}}\boldsymbol{r}_{jk'}^{\boldsymbol{X}'T}. \tag{21}$$

Since $\boldsymbol{Z}(t) = \boldsymbol{F}(\boldsymbol{Y}(t), \boldsymbol{\alpha}) + \mathbf{f}_\phi(\boldsymbol{X}(t))$, the observation $\boldsymbol{Z}$ in the model follows the Gaussian distribution

$$\begin{bmatrix}\boldsymbol{Z}(t)\\ \boldsymbol{Z}(t')\end{bmatrix} \sim \mathcal{N}(\begin{bmatrix}\boldsymbol{F}(\boldsymbol{Y}(t), \boldsymbol{\alpha})\\ \boldsymbol{F}(\boldsymbol{Y}(t'), \boldsymbol{\alpha})\end{bmatrix}, K_{\mathbf{f}_\phi}(\boldsymbol{X}(t), \boldsymbol{X}(t'))). \tag{22}$$

This completes the proof. □

Observation data regime We fix L time stamps with $0 = t_1 < t_2 < \cdots t_L = T$ on $[0, T]$ and obtain the trajectory data $\{\boldsymbol{Y}(t_l), \boldsymbol{Z}_{\sigma^2}(t_l) : 1 \leq l \leq L\}$ as one training instance, where σ^2 denotes the unknown variance of additive Gaussian noise specified below. Furthermore, we hold the following two assumptions on training data of M training instances:

1. The M initial conditions $\{\boldsymbol{Y}^{(m)}(0) : 1 \leq m \leq M\}$ are drawn randomly from a probability measure $\boldsymbol{\mu}_0 = [\mu_0^{\boldsymbol{X}}, \mu_0^{\dot{\boldsymbol{X}}}]^T$ on $\mathbb{R}^{2dN}$.
2. The accelerations $\{\boldsymbol{Z}^{(m)}(t_l) : 1 \leq l \leq N, 1 \leq m \leq M\}$ are observed with i.i.d additive Gaussian noise $\boldsymbol{\epsilon} \sim \mathcal{N}(\mathbf{0}, \sigma^2 I_{dN\times dN})$, so that the data is denoted by $\boldsymbol{Z}_{\sigma^2}^{(m)}(t_l)$.

Remark 1. *The Gaussian assumptions on observational noise are necessary for us to derive the closed formulas of the estimators. In the actual algorithm, we can approximate the velocity and acceleration from the position data. The resulting estimators will be approximations of the estimators obtained in the ideal data regime.*

Applying Lemma 2, we now derive the negative log marginal likelihood for training parameters $\boldsymbol{\alpha}$, θ, and σ, with given observational data as specified above.

Proposition 3. *Denote $\boldsymbol{Y}^{(m,l)} = \boldsymbol{Y}^{(m)}(t_l)$ and $\boldsymbol{Z}_{\sigma^2}^{(m,l)} = \boldsymbol{Z}^{(m)}(t_l) + \epsilon^{(m,l)}$ with i.i.d noise $\boldsymbol{\epsilon}^{(m,l)} \sim \mathcal{N}(0, \sigma^2 I_{dN\times dN})$. Suppose we are given the training data set $(\mathbb{Y}_M, \mathbb{Z}_{\sigma^2,M}) := \{(\boldsymbol{Y}^{(m,l)}, \boldsymbol{Z}_{\sigma^2}^{(m,l)})\}_{m,l=1}^{M,L}$ for $M, L \in \mathbb{N}$, such that*

$$\boldsymbol{Z}_{\sigma^2}^{(m,l)} = \boldsymbol{F}(\boldsymbol{Y}^{(m,l)}, \boldsymbol{\alpha}) + \mathbf{f}_\phi(\boldsymbol{X}^{(m,l)}) + \boldsymbol{\epsilon}^{(m,l)}, \tag{23}$$

with $\boldsymbol{F}(\cdot, \boldsymbol{\alpha})$, $\mathbf{f}_\phi$ defined in Table 1. Then the negative log marginal likelihood of $\mathbb{Z}_{\sigma^2,M}$ given $\mathbb{Y}_M$ and parameters $\boldsymbol{\alpha}$, θ, σ satisfies

$$\begin{aligned} - &\quad \log p(\mathbb{Z}_{\sigma^2,M}|\mathbb{Y}_M, \boldsymbol{\alpha}, \theta, \sigma^2) &(24)\\ = &\quad \frac{1}{2}(\mathbb{Z}_{\sigma^2,M} - \boldsymbol{F}(\mathbb{Y}_M, \boldsymbol{\alpha}))^T(K_{\mathbf{f}_\phi}(\mathbb{X}_M, \mathbb{X}_M; \theta) + \sigma^2 I)^{-1}(\mathbb{Z}_{\sigma^2,M} - \boldsymbol{F}(\mathbb{Y}_M, \boldsymbol{\alpha}))\\ &\quad + \frac{1}{2}\log|K_{\mathbf{f}_\phi}(\mathbb{X}_M, \mathbb{X}_M; \theta) + \sigma^2 I| + \frac{dNML}{2}\log 2\pi. &(25)\end{aligned}$$

where $K_{\mathbf{f}_\phi}(\mathbb{X}_M, \mathbb{X}_M; \theta)$ denotes the covariance matrix between $\mathbf{f}_\phi(\mathbb{X}_M)$ and $\mathbf{f}_\phi(\mathbb{X}_M)$, I is the identity matrix of consistent size.

Proof. Using Lemma 2, since $\epsilon^{(m,l)}$ is i.i.d Gaussian noise and is independent of the initial distributions, we have that

$$\mathbb{Z}_{\sigma^2,M} \sim \mathcal{N}(\boldsymbol{F}(\mathbb{Y}_M, \boldsymbol{\alpha}), K_{\mathbf{f}_\phi}(\mathbb{X}_M, \mathbb{X}_M; \theta) + \sigma^2 I_{dNML}), \tag{26}$$

where the mean vector $\boldsymbol{F}(\mathbb{Y}_M, \boldsymbol{\alpha}) = \text{vec}((\boldsymbol{F}(\boldsymbol{Y}^{(m,l)}, \boldsymbol{\alpha}))_{m,l=1}^{M,L}) \in \mathbb{R}^{dNML}$, and the covariance matrix $K_{\mathbf{f}_\phi}(\mathbb{X}_M, \mathbb{X}_M; \theta) = \left(\text{Cov}(\mathbf{f}_\phi(\boldsymbol{X}^{(m,l)}), \mathbf{f}_\phi(\boldsymbol{X}^{(m',l')}))\right)_{m,m',l,l'=1}^{M,M,L,L}$ can be computed componentwise using (15). According to the properties of the Gaussian distribution, given $\mathbb{Y}$ and parameters $\boldsymbol{\alpha}$, θ, σ, we have the negative log marginal likelihood function as shown in (25). □

As mentioned earlier, we can apply the gradient-based method (Liu and Nocedal, 1989), to minimize the negative log marginal likelihood and solve for the hyper-parameters $(\boldsymbol{\alpha}, \theta, \sigma)$.

Proposition 4. *Let* $\boldsymbol{\gamma} = (K_{\mathbf{f}_\phi}(\mathbb{X}_M, \mathbb{X}_M; \theta) + \sigma^2 I)^{-1}(\mathbb{Z}_{\sigma^2,M} - \boldsymbol{F}(\mathbb{Y}_M, \boldsymbol{\alpha}))$. *The partial derivatives of the marginal likelihood w.r.t. the parameters* $\boldsymbol{\alpha}, \theta$, *and* σ *can be computed as follows:*

$$\frac{\partial}{\partial \boldsymbol{\alpha}_i} \log p(\mathbb{Z}_{\sigma^2,M} | \mathbb{Y}_M, \boldsymbol{\alpha}, \theta, \sigma^2) = \boldsymbol{\gamma}^T \frac{\partial \boldsymbol{F}(\mathbb{Y}_M, \boldsymbol{\alpha})}{\partial \boldsymbol{\alpha}_i}. \tag{27}$$

$$\frac{\partial}{\partial \theta_j} \log p(\mathbb{Z}_{\sigma^2,M} | \mathbb{Y}_M, \boldsymbol{\alpha}, \theta, \sigma^2) = \frac{1}{2}\text{Tr}\left((\boldsymbol{\gamma}\boldsymbol{\gamma}^T - (K_{\mathbf{f}_\phi}(\mathbb{X}_M, \mathbb{X}_M; \theta) + \sigma^2 I)^{-1}) \frac{\partial K_{\mathbf{f}_\phi}(\mathbb{X}_M, \mathbb{X}_M; \theta)}{\partial \theta_j}\right). \tag{28}$$

$$\frac{\partial}{\partial \sigma} \log p(\mathbb{Z}_{\sigma^2,M} | \mathbb{Y}_M, \boldsymbol{\alpha}, \theta, \sigma^2) = \text{Tr}\left((\boldsymbol{\gamma}\boldsymbol{\gamma}^T - (K_{\mathbf{f}_\phi}(\mathbb{X}_M, \mathbb{X}_M; \theta) + \sigma^2 I)^{-1})\right) \sigma. \tag{29}$$

After optimization of the log likelihood using the computed partial derivatives, we obtain maximum likelihood estimators denoted by $\hat{\theta}$, $\hat{\boldsymbol{\alpha}}$, and $\hat{\sigma}$.

Next, we show the detailed derivation of our estimators for the prediction of $\phi(r^*)$ at $r^* \in [0, R]$ if θ, $\boldsymbol{\alpha}$, and σ are known.

Theorem 5. *Suppose the parameters* θ, $\boldsymbol{\alpha}$, *and* σ *are known and we are given the training data set* $(\mathbb{Y}_M, \mathbb{Z}_{\sigma^2,M}) := \{(\boldsymbol{Y}^{(m,l)}, \boldsymbol{Z}_{\sigma^2}^{(m,l)})\}_{m,l=1}^{M,L}$ *defined in Proposition 3, Then for any* $r^* \in [0, R]$, $\phi(r^*)$ *satisfies*

$$p(\phi(r^*) | \mathbb{Y}_M, \mathbb{Z}_{\sigma^2,M}) \sim \mathcal{N}(\bar{\phi}^*, \text{Var}(\phi^*)), \tag{30}$$

where

$$\bar{\phi}^* = K_{\phi,\mathbf{f}_\phi}(r^*, \mathbb{X}_M)(K_{\mathbf{f}_\phi}(\mathbb{X}_M, \mathbb{X}_M) + \sigma^2 I)^{-1}(\mathbb{Z}_{\sigma^2,M} - \boldsymbol{F}(\mathbb{Y}_M, \boldsymbol{\alpha})), \tag{31}$$

$$\text{Var}(\phi^*) = K_\theta(r^*, r^*) - K_{\phi,\mathbf{f}_\phi}(r^*, \mathbb{X}_M)(K_{\mathbf{f}_\phi}(\mathbb{X}_M, \mathbb{X}_M) + \sigma^2 I)^{-1} K_{\mathbf{f}_\phi,\phi}(\mathbb{X}_M, r^*). \tag{32}$$

and $K_{\mathbf{f}_\phi,\phi}(\mathbb{X}_M, r^*) = K_{\phi,\mathbf{f}_\phi}(r^*, \mathbb{X}_M)^T$ *denotes the covariance matrix between* $\mathbf{f}_\phi(\mathbb{X}_M)$ *and* $\phi(r^*)$.

Proof. Since $\mathbf{f}_\phi(\mathbb{X}_M)$ is defined componentwisely by (19), for any $r^* \in [0, R]$, we have that

$$\begin{bmatrix} \mathbf{f}_\phi(\mathbb{X}_M) \\ \phi(r^*) \end{bmatrix} \sim \mathcal{N}\left(0, \begin{bmatrix} K_{\mathbf{f}_\phi}(\mathbb{X}_M, \mathbb{X}_M) & K_{\mathbf{f}_\phi,\phi}(\mathbb{X}_M, r^*) \\ K_{\phi,\mathbf{f}_\phi}(r^*, \mathbb{X}_M) & K_\theta(r^*, r^*) \end{bmatrix}\right), \tag{33}$$

where $K_{\mathbf{f}_\phi}(\mathbb{X}_M, \mathbb{X}_M)$ is the covariance matrix between $\mathbf{f}_\phi(\mathbb{X}_M)$ and $\mathbf{f}_\phi(\mathbb{X}_M)$ as we defined in Proposition 3, and $K_{\mathbf{f}_\phi,\phi}(\mathbb{X}_M, r^*) = K_{\phi,\mathbf{f}_\phi}(r^*, \mathbb{X}_M)^T$ is the covariance matrix between $\mathbf{f}_\phi(\mathbb{X}_M)$ and $\phi(r^*)$, i.e., $K_{\mathbf{f}_\phi,\phi}(\mathbb{X}_M, r^*) = (\text{Cov}(\mathbf{f}_\phi(\boldsymbol{X}^{(m,l)}), \phi(r^*)))_{m,l=1}^{M,L}$ and the i-th component of $\text{Cov}(\mathbf{f}_\phi(\boldsymbol{X}^{(m,l)}), \phi(r^*))$ is computed by

$$\text{Cov}([\mathbf{f}_\phi(\boldsymbol{X}^{(m,l)})]_i, \phi(r^*)) = \frac{1}{N}\sum_{k \neq i} K_\theta(r_{ik}^{\boldsymbol{X}}, r^*) \boldsymbol{r}_{ik}^{\boldsymbol{X}}. \tag{34}$$

Note that $\boldsymbol{Z}_{\sigma^2}^{(m,l)} = \boldsymbol{F}(\boldsymbol{Y}^{(m,l)}, \boldsymbol{\alpha}) + \mathbf{f}_\phi(\boldsymbol{X}^{(m,l)}) + \epsilon^{(m,l)}$ with i.i.d noise $\boldsymbol{\epsilon}^{(m,l)} \sim \mathcal{N}(0, \sigma^2 I_{dN})$ for all (m, l), so we have

$$\begin{bmatrix} \mathbb{Z}_{\sigma^2,M} - F(\mathbb{Y}_M, \boldsymbol{\alpha}) \\ \phi(r^*) \end{bmatrix} \sim \mathcal{N}\left(0, \begin{bmatrix} K_{\mathbf{f}_\phi}(\mathbb{X}_M, \mathbb{X}_M) + \sigma^2 I_{dNML} & K_{\mathbf{f}_\phi,\phi}(\mathbb{X}_M, r^*) \\ K_{\phi,\mathbf{f}_\phi}(r^*, \mathbb{X}_M) & K_\theta(r^*, r^*) \end{bmatrix}\right), \tag{35}$$

Therefore, based on the properties of the joint Gaussian distribution (see Lemma 27), conditioning on $(\mathbb{Y}_M, \mathbb{Z}_{\sigma^2,M})$, we have that

$$p(\phi(r^*)|\mathbb{Y}_M, \mathbb{Z}_{\sigma^2,M}, r^*) \sim \mathcal{N}(\bar{\phi}^*, var(\phi^*)), \tag{36}$$

where $\bar{\phi}^*$ and $\mathrm{Var}(\phi^*)$ are defined as in (31) and (32). □

We would like point out that in practice, we use $\hat{\theta}$, $\hat{\boldsymbol{\alpha}}$, and $\hat{\sigma}$ learning from the training set (as mentioned above) in (31) and (32) to predict $\phi(r^*)$. The kernel used is in fact $\widehat{K} = K_{\hat{\theta}}$.

Moreover, if we consider the case when $m_i \equiv 0$, and $F_i(\boldsymbol{x}_i(t), \dot{\boldsymbol{x}}_i(t), \boldsymbol{\alpha}) = -\dot{\boldsymbol{x}}_i(t)$ all for $i = 1 \ldots, N$ in (12), then it becomes the first-order systems (1), and we can derive the following corollary as we have shown in (8) and (9).

Corollary 6. *Suppose the parameters θ and σ are known, and we are given the training data set $\mathbb{Y}_{\sigma^2,M} = \{\mathbb{X}_M, \mathbb{V}_{\sigma^2,M}\}$ from the first-order systems (1), then for any $r^* \in [0, R]$, $\phi(r^*)$ satisfies*

$$p(\phi(r^*)|\mathbb{Y}_{\sigma^2,M}) \sim \mathcal{N}(\bar{\phi}^*, \mathrm{Var}(\phi^*)), \tag{37}$$

$$\bar{\phi}^* = K_{\phi,\mathbf{f}_\phi}(r^*, \mathbb{X}_M)(K_{\mathbf{f}_\phi}(\mathbb{X}_M, \mathbb{X}_M) + \sigma^2 I)^{-1}\mathbb{V}_{\sigma^2,M}, \tag{38}$$

$$\mathrm{Var}(\phi^*) = K(r_*, r_*) - K_{\phi,\mathbf{f}_\phi}(r^*, \mathbb{X}_M)(K_{\mathbf{f}_\phi}(\mathbb{X}_M, \mathbb{X}_M) + \sigma^2 I)^{-1}K_{\mathbf{f}_\phi,\phi}(\mathbb{X}_M, r^*). \tag{39}$$

3 Error analysis

Numerical results in section 4 show that $\boldsymbol{\alpha}$ and σ^2 were accurately recovered from small amounts of noisy data in the training step. In this section, we shall focus on the prediction step of our GP-based learning approach: suppose the interaction kernel is the only unknown term in the governing equation, and our goal is to establish a rigorous quantitative framework which analyzes the error of the posterior mean (31) that approximates ϕ and the marginal posterior variance when L is fixed and $M \to \infty$.

3.1 Preliminaries

Assumption 7. *The distribution of initial conditions μ_0 is compactly supported on $\mathbb{R}^{dN}$.*

Recall that K is a Mercer kernel that is defined on $[0, R] \times [0, R]$ and $\mathcal{H}_K$ is the RKHS associated to K.

Lemma 8. *Suppose $\kappa^2 = \sup_{r\in[0,R]} K(r, r) < \infty$. Then we have that, for any $\varphi \in \mathcal{H}_K$, there holds $\|\varphi\|_\infty \le \kappa\|\varphi\|_{\mathcal{H}_K}$.*

Proof. By the reproducing property of K, we have that

$$|\varphi(r)| = |\langle\varphi, K_r\rangle_{\mathcal{H}_K}| \le \|\varphi\|_{\mathcal{H}_K}\|K_r\|_{\mathcal{H}_K} \le \kappa\|\varphi\|_{\mathcal{H}_K}.$$

The conclusion follows. □

Remark 2. *The reproducing property implies that functions in $\mathcal{H}_K$ are continuous. In general, the smoothness of the Mercer kernel is closely related to the smoothness of functions in $\mathcal{H}_K$. Let $C^s([0,R])$ be the space of all functions defined on $[0,R]$ whose partial derivatives up to order s are continuous with the norm $\|f\|_{C^s} = \sum_{|\alpha|\le s} \|D^\alpha f\|_\infty$, and $C^{s+\epsilon}([0,R])$ denotes the subspace of $C^s([0,R])$ of functions with these partial derivatives to be Hölder ϵ on $[0,R]$. In (Smale and Zhou, 2007), it has been shown that if $K \in C^{2s+\epsilon}([0,R]\times[0,R])$ with $0<\epsilon<2$, the inclusion $\mathcal{H}_K \subset C^{2s+\frac{\epsilon}{2}}([0,R]\times[0,R])$ is well-defined, bounded and*

$$\|\varphi\|_{C^s} \le 4^s \|K\|_{C^{2s}}^{\frac{1}{2}} \|\varphi\|_{\mathcal{H}_K}, \forall \varphi \in \mathcal{H}_K.$$

We introduce an important measure that will be crucial in our theoretical analysis. Note that the observational variables for ϕ consist of pairwise distances. In (Lu et al., 2019), a probability measure on $\mathbb{R}^+$ that encodes the information about the dynamics marginalized to pairwise distance was introduced as

$$\rho_T^L(dr) := \frac{1}{\binom{N}{2}} \sum_{l=1}^{L} \Big[\sum_{i,i'=1, i<i'}^{N} \mathbb{E}_{\mu_0}[\delta_{r_{ii'}(t_l)}(dr)], \Big], \tag{40}$$

where δ is the Dirac δ distribution and $r_{ii'}(t_l) := |\boldsymbol{x}_i(t_l) - \boldsymbol{x}_{i'}(t_l)|$, so that $\mathbb{E}_{\mu_0}[\delta_{r_{ii'}(t)}(dr)]$ is the distribution of the random variable $r_{ii'}(t)$ being the position of particle i at time t. Note that it is on the support of ρ_T^L that ϕ could be learned. The probability measure ρ_T^L can be thought of as an "occupancy" measure, in the sense that for any interval $I \subset \mathbb{R}^+$, $\rho_T^L(I)$ is the probability of seeing a pair of agents at a distance between them equal to a value in I, averaged over the observation time. It measures how much regions of $\mathbb{R}^+$ on average (over the observed times and with respect to the distribution μ_0 of the initial conditions) are explored by the dynamical system.

Without loss of generality, we assume that ρ_T^L is non-degenerate on $[0,R]$[1]. Due to the structure of the equation, we introduce a positive measure that appears naturally in estimating the error of estimators:

$$\tilde{\rho}_T^L(r) = r^2 \rho_T^L(dr) \llcorner [0,R], r \in \mathbb{R}^+. \tag{41}$$

One can refer to Section 2.1 of (Lu et al., 2021) for the analytical study of measures.

3.2 Learning as a statistical inverse problem

For easy presentation, we restrict our attention to first-order systems, which is a special case of second-order systems by assuming the masses of the agents are zero:

$$\dot{\boldsymbol{X}}(t) = \mathbf{f}_\phi(\boldsymbol{X}(t)). \tag{42}$$

Our analysis can be extended to second-order systems with (known) non-collective force terms with very slight modifications. For first-order systems, we are given the noisy trajectory data

$$\boldsymbol{V}_{\sigma^2}^{(m,l)} := \mathbf{f}_\phi(\boldsymbol{X}^{(m,l)}) + \boldsymbol{\epsilon}^{(m,l)}, \quad m = 1, \cdots, M;\ l = 1, \cdots, L, \tag{43}$$

where $\boldsymbol{X}^{(m,l)} = \boldsymbol{X}^{(m)}(t_l)$ and $\boldsymbol{\epsilon}^{(m,l)}$ is the additive Gaussian noise with variance $\sigma^2 I$ independent of μ_0. The trajectory data is indeed of the type needed for the nonparametric regression of $\mathbf{f}_\phi$. One can construct an empirical quadratic risk functional

$$\frac{1}{ML} \sum_{m,l=1}^{M,L} \|\boldsymbol{V}_{\sigma^2}^{(m,l)} - \boldsymbol{f}(\boldsymbol{X}^{(m,l)})\|^2 \tag{44}$$

[1]For example, we can choose $\mu_0 := \mathrm{Unif}[-\frac{R}{2}, \frac{R}{2}]^{dN}$. Then $\mathrm{Supp}(\rho_T^1) = [0,R]$ and $\mathrm{Supp}(\rho_T^1) \subset \mathrm{Supp}(\rho_T^L)$ for $L > 1$.

to find the least square estimator of $\mathbf{f}_\phi$ over a hypothesis function space.

In this paper, we are interested in the data regime: L fixed, $M \to \infty$. In the case of $M = \infty$, the expectation of risk functional (44) becomes

$$\|\mathbf{f}_\phi(\boldsymbol{X}) - \boldsymbol{f}(\boldsymbol{X})\|^2_{L^2(\rho_{\boldsymbol{X}})} \tag{45}$$

where the probability measure $\rho_{\boldsymbol{X}}$ is defined by

$$\rho_{\boldsymbol{X}} := \mathbb{E}_{\boldsymbol{X}(0)\sim\mu_0}\left[\frac{1}{L}\sum_{l=1}^{L}\delta_{\boldsymbol{X}(t_l)}\right]; \tag{46}$$

δ is the Dirac δ distribution; $\boldsymbol{X}(t_l) \in \mathbb{R}^{dN}$ is the position vector of all agents at time t_l. Therefore one can find an unbiased estimator of $\mathbf{f}_\phi$ if the regression function space is $L^2(\mathbb{R}^{dN}; \boldsymbol{\rho}_{\boldsymbol{X}}; \mathbb{R}^{dN})$. However, the classical nonparametric regression theory (Györfi et al., 2006) implies that the optimal minimax convergence rate of least square estimators is cursed by the ambient dimension dN, which significantly restricts their usability as soon as, say, $dN \geq 10$. It is necessary to exploit the structure of the governing equation encoded in $\mathbf{f}$ and shift our regression target to ϕ. This will become an inverse problem as shown below.

Operator representations of the learning problem Below, we introduce an operator A to represent the learning problem and specify function spaces on which A is a bounded linear operator.

Proposition 9. *Let A be an operator defined by*

$$A\varphi = \mathbf{f}_\varphi \tag{47}$$

where $\varphi \in \mathcal{H}_K$ and $\mathbf{f}_\varphi$ is given in (42) specifying the interaction force. Then A is a linear bounded operator that maps $\mathcal{H}_K$ to $L^2(\mathbb{R}^{dN}; \rho_{\boldsymbol{X}}; \mathbb{R}^{dN})$ with $\|A\| \leq \kappa R$. The adjoint operator A^* satisfies

$$A^* g = \int_{\boldsymbol{X}} \frac{1}{N^2} \sum_{i=1, i'\neq i}^{N} K_{r_{ii'}} \langle \boldsymbol{r}_{ii'}, g_i(\boldsymbol{X})\rangle \, d\rho_{\boldsymbol{X}}, \tag{48}$$

where $g = [g_1^T, \cdots, g_N^T]^T$ with $g_i : \mathbb{R}^{dN} \to \mathbb{R}^d$. As a consequence, the operator B, defined by

$$B\varphi := A^*A\varphi = \frac{1}{N^3}\int_{\boldsymbol{X}} \sum_{i,i',i''} K_{r_{ii'}} \langle \varphi, K_{r_{ii''}}\rangle_{\mathcal{H}_K} \langle \boldsymbol{r}_{ii'}, \boldsymbol{r}_{ii''}\rangle \, d\rho_{\boldsymbol{X}}, \tag{49}$$

is a trace class operator mapping $\mathcal{H}_K$ to $\mathcal{H}_K$. In addition, B can be also viewed as a bounded linear operator from $L^2(\tilde{\rho}_T^L)$ to $L^2(\tilde{\rho}_T^L)$.

To prove the Proposition above, we first state the following Lemma:

Lemma 10. *If μ_0 is compactly supported, then for $1 \leq i, i' \leq N$, we have $\boldsymbol{r}_{ii'}(\boldsymbol{X}) = \boldsymbol{x}_{i'} - \boldsymbol{x}_i \in L^2(\mathbb{R}^{dN}; \rho_{\boldsymbol{X}}; \mathbb{R}^d) = \{\boldsymbol{f} : \mathbb{R}^{dN} \to \mathbb{R}^d | \int_{\mathbb{R}^{dN}} \|\boldsymbol{f}(\boldsymbol{X})\|^2 d\rho_{\boldsymbol{X}} < \infty\}$.*

The proof of the above lemma is similar to the proof of Proposition 2 in (Lu et al., 2020). It utilizes the standard dynamical system techniques to show the trajectory starting from any $\boldsymbol{X}(0)$ sampled from μ_0 is inside a bounded region in $\mathbb{R}^{dN}$ within a finite time interval $[0, T]$. Consequently, $\boldsymbol{r}_{ii'}$ is bounded and therefore lies in the L^2 space. One may generalize the argument to include distributions with a fast decay, such as the Gaussian distributions. We are now ready to prove Proposition 9.

Proof of Proposition 9. Lemma 8 implies that $\mathcal{H}_K$ can be naturally embedded as a subspace of $L^2(\tilde{\rho}_T^L)$. Using Lemma 28, we have that

$$\|A\varphi\|^2_{L^2(\rho_{\boldsymbol{X}})} = \|\mathbf{f}_\varphi\|^2_{L^2(\rho_{\boldsymbol{X}})} \leq \frac{N-1}{N}\|\varphi\|^2_{L^2(\tilde{\rho}_T^L)} < R^2\|\varphi\|^2_\infty \leq \kappa^2 R^2 \|\varphi\|^2_{\mathcal{H}_K}. \tag{50}$$

This shows that A is a bounded linear operator mapping $\mathcal{H}_K$ to $L^2(\mathbb{R}^{dN}; \rho_{\boldsymbol{X}}; \mathbb{R}^{dN})$ and $\|A\| \leq \kappa R$.

Next, we prove (48). We first show that the map for each (i, i'), the map

$$\boldsymbol{X} \to K_{r_{ii'}} \in \mathcal{H}_K$$

is continuous since $\|K_{r_{ii'}} - K_{r'_{ii'}}\|^2_{\mathcal{H}_K} = K(r_{ii'}, r_{ii'}) + K(r'_{ii'}, r'_{ii'}) - 2K(r_{ii'}, r'_{ii'})$ for all $r_{ii'} = \|\boldsymbol{x}_i - \boldsymbol{x}_{i'}\|$, $r'_{ii'} = \|\boldsymbol{x}'_i - \boldsymbol{x}'_{i'}\|$, and $\boldsymbol{X}, \boldsymbol{X}' \in \mathbb{R}^{dN}$, and both K and $\|\cdot\|$ are continuous. Hence given a function $g \in L^2(\mathbb{R}^{dN}; \rho_{\boldsymbol{X}}; \mathbb{R}^{dN})$, the map

$$\boldsymbol{X} \to \frac{1}{N^2}\sum_{i=1, i'\neq i}^N K_{r_{ii'}}\langle \boldsymbol{r}_{ii'}, g_i(\boldsymbol{X})\rangle$$

is measurable from $\mathbb{R}^{dN}$ to $\mathcal{H}_K$. Moreover,

$$\|\frac{1}{N^2}\sum_{i=1, i'\neq i}^N K_{r_{ii'}}\langle \boldsymbol{r}_{ii'}, g_i(\boldsymbol{X})\rangle\|_{\mathcal{H}_K} \leq \frac{\kappa}{N^2}\sum_{i=1, i'\neq i}^N |\langle \boldsymbol{r}_{ii'}, g_i(\boldsymbol{X})\rangle|.$$

By Lemma 10, we have that both $\boldsymbol{r}_{ii'}, g_i(\boldsymbol{X}) \in L^2(\mathbb{R}^{dN}; \rho_{\boldsymbol{X}}; \mathbb{R}^d)$. By Hölder's inequality (or Cauchy-Schwartz inequality), $\langle \boldsymbol{r}_{ii'}, g_i(\boldsymbol{X})\rangle$ is in $L^1(\mathbb{R}^{dN}; \rho_{\boldsymbol{X}}; \mathbb{R})$, and hence $\frac{1}{N^2}\sum_{i=1, i'\neq i}^N K_{r_{ii'}}\langle \boldsymbol{r}_{ii'}, g_i(\boldsymbol{X})\rangle$ is integrable as a vector-valued map.

Finally, for any $\psi \in \mathcal{H}_K$,

$$\begin{aligned}
\langle A\psi, g\rangle_{L^2(\rho_{\boldsymbol{X}})} &= \frac{1}{N}\sum_{i=1}^N \int_{\boldsymbol{X}} \langle [\mathbf{f}_\psi(\boldsymbol{X})]_i, g_i(\boldsymbol{X})\rangle \, d\rho_{\boldsymbol{X}}(\boldsymbol{X}) \\
&= \frac{1}{N^2}\sum_{i=1}^N\sum_{i'=1}^N \int_{\boldsymbol{X}} \psi(r_{ii'})\langle \boldsymbol{r}_{ii'}, g_i(\boldsymbol{X})\rangle \, d\rho_{\boldsymbol{X}}(\boldsymbol{X}) \\
&= \frac{1}{N^2}\sum_{i=1}^N\sum_{i'=1}^N \int_{\boldsymbol{X}} \langle \psi, K_{r_{ii'}}\rangle_{\mathcal{H}_K}\langle \boldsymbol{r}_{ii'}, g_i(\boldsymbol{X})\rangle \, d\rho_{\boldsymbol{X}}(\boldsymbol{X}) \\
&= \langle \psi, \frac{1}{N^2}\sum_{i=1}^N\sum_{i'=1}^N \int_{\boldsymbol{X}} K_{r_{ii'}}\langle \boldsymbol{r}_{ii'}, g_i(\boldsymbol{X})\rangle \, d\rho_{\boldsymbol{X}}(\boldsymbol{X})\rangle_{\mathcal{H}_K} = \langle \psi, A^* g\rangle_{\mathcal{H}_K},
\end{aligned}$$

so by the uniqueness of the integral, (48) holds. Equation (49) follows from (48) by direct calculations and the fact that the integral commutes with the scalar product.

We now prove that B is a trace class operator, i.e. to show that $\mathrm{Tr}(|B|) < \infty$, where $|B| = \sqrt{B^*B}$. Since B is positive, we have $|B| = B$. Therefore it is equivalent to show $\mathrm{Tr}(B) < \infty$.

$$\begin{aligned}
\mathrm{Tr}(B) = \mathrm{Tr}(A^*A) &= \sum_n \langle A^*Ae_n, e_n\rangle_{\mathcal{H}_K} = \sum_n \langle Ae_n, Ae_n\rangle_{L^2(\rho_{\boldsymbol{X}})} \\
&= \sum_n \|\mathbf{f}_{e_n}(\boldsymbol{X})\|^2_{L^2(\rho_{\boldsymbol{X}})} < \sum_n \|e_n\|^2_{L^2(\tilde{\rho}_T^L)} \\
&\leq R^2 \sum_n \|e_n\|^2_{L^2(\rho_T^L)} = R^2 \int \langle K_r, K_r\rangle_{\mathcal{H}_K} \, d\rho_T^L(r) \leq \kappa^2 R^2,
\end{aligned}$$

Table 2: Notations in the empirical version

Notation	Definition
$\mathbb{X}_M \in \mathbb{R}^{dNML}$	vectorization of $\{\boldsymbol{X}^{(m,l)})\}_{m,l=1}^{M,L}$
$A_M : \mathcal{H}_K \to \mathbb{R}^{dNML}$	$A_M\varphi = \mathbf{f}_\varphi(\mathbb{X}_M)$
$A_M^* : \mathbb{R}^{dNML} \to \mathcal{H}_K$	adjoint operator of A_M
$B_M : \mathcal{H}_K \to \mathcal{H}_K$	$B_M = A_M^* A_M$
$\mathcal{E}^{\lambda,M}(\cdot)$	the regularized empirical risk functional (see (65))
$\phi_{\mathcal{H}_K}^{\lambda,M}$	minimizer of $\mathcal{E}^{\lambda,M}(\cdot)$ in $\mathcal{H}_K$

where we used Lemma 28 to show the inequality in the second line and

$$\langle K_r, K_r\rangle_{\mathcal{H}_K} = \langle\sum_n \langle K_r, e_n\rangle_{\mathcal{H}_K} e_n, K_r\rangle_{\mathcal{H}_K} = \langle\sum_n \langle K_r, e_n\rangle_{\mathcal{H}_K} e_n, K_r\rangle_{\mathcal{H}_K} = \sum_n e_n^2(r).$$

Lastly, we show B can be viewed as a bounded operator on $L^2(\tilde{\rho}_T^L)$. Assume that $\varphi \in L^2(\tilde{\rho}_T^L)$, we have the identity that $B\varphi(r) = \langle \mathbf{f}_\varphi(\boldsymbol{X}), \mathbf{f}_{K_r}(\boldsymbol{X})\rangle_{L^2(\rho_{\boldsymbol{X}})}$. We obtain that

$$\begin{aligned}
|B\varphi(r)| &\le \|\mathbf{f}_\varphi(\boldsymbol{X})\|_{L^2(\rho_{\boldsymbol{X}})} \|\mathbf{f}_{K_r}(\boldsymbol{X})\|_{L^2(\rho_{\boldsymbol{X}})} \\
&\le \frac{N-1}{N} \|\varphi\|_{L^2(\tilde{\rho}_T^L)} \|K_r\|_{L^2(\tilde{\rho}_T^L)} \\
&\le \frac{N-1}{N} \|\varphi\|_{L^2(\tilde{\rho}_T^L)} R \|K_r\|_{L^2(\rho_T^L)} \\
&\le \frac{N-1}{N} \|\varphi\|_{L^2(\tilde{\rho}_T^L)} R \|K_r\|_\infty \\
&\le \frac{N-1}{N} \|\varphi\|_{L^2(\tilde{\rho}_T^L)} \kappa R \|K_r\|_{\mathcal{H}_K} \\
&\le \frac{N-1}{N} \|\varphi\|_{L^2(\tilde{\rho}_T^L)} \kappa^2 R. \qquad (51)
\end{aligned}$$

where the last inequality follows from $\|K_r\|_{\mathcal{H}_K} = \sqrt{K(r,r)} \le \kappa$.

As a result, $B\varphi \in L^2(\tilde{\rho}_T^L)$, and B can be viewed as a bounded linear operator from $L^2(\tilde{\rho}_T^L)$ to $L^2(\tilde{\rho}_T^L)$ with $\|B\|_{L^2(\tilde{\rho}_T^L)} \le \kappa^2 R^2$. □

When $M = \infty$, our learning problem is then equivalent to solving a linear operator equation

$$A\varphi = \mathbf{f}_\phi. \qquad (52)$$

and it is, therefore, a linear inverse problem over possibly infinite dimensional space. In particular, when $L = 1$, our learning problem becomes a standard statistical inverse problem with a random and noisy observation scheme (Blanchard and Mücke, 2018).

In the case of finite data, i.e., $M < \infty$, we introduce an empirical version of A, denoted by A_M, see also in Table 2, to represent the learning problem.

Proposition 11. *Given the empirical noisy trajectory data with the vectorized notation* $\mathbb{Y}_{\sigma^2,M} = \{\mathbb{X}_M, \mathbb{V}_{\sigma^2,M}\}$*, we define the sampling operator* $A_M : \mathcal{H}_K \to \mathbb{R}^{dNML}$ *by*

$$A_M\varphi = \mathbf{f}_\varphi(\mathbb{X}_M) := \mathrm{Vec}(\{\mathbf{f}_\varphi(\boldsymbol{X}^{(m,l)})\}_{m,l=1}^{M,L}), \qquad (53)$$

where $\mathbb{R}^{dNML}$ is equipped with the inner product defined in (11). *The adjoint operator A_M^* is a finite rank operator. For any $\mathbb{W}$ in $\mathbb{R}^{dNML}$, let $\mathbb{W}_{m,l,i} \in \mathbb{R}^d$ denote the i-th component of the (m,l)-th block of $\mathbb{W}$. Then we have*

$$A_M^* \mathbb{W} = \frac{1}{LM} \sum_{l,m=1}^{L,M} \sum_{i=1,i'\neq i}^{N} \frac{1}{N^2} K_{r_{ii'}^{(m,l)}} \langle \boldsymbol{r}_{ii'}^{(m,l)}, \mathbb{W}_{m,l,i} \rangle.$$

For any function $\varphi \in \mathcal{H}_K$, we have that

$$B_M \varphi := A_M^* A_M \varphi = \frac{1}{LM} \sum_{l,m=1}^{L,M} \left(\sum_{i=1,i',i''\neq i}^{N} \frac{1}{N^3} K_{r_{ii'}^{(m,l)}} \langle \varphi, K_{r_{ii''}^{(m,l)}} \rangle_{\mathcal{H}_K} \langle \boldsymbol{r}_{ii'}^{(m,l)}, \boldsymbol{r}_{ii''}^{(m,l)} \rangle \right).$$

Proof of Proposition 11. The formula of A_M^* can be derived by using the identity $\langle A_M \varphi, \boldsymbol{w} \rangle = \langle \varphi, A_M^* \boldsymbol{w} \rangle_{\mathcal{H}_K}$. The direct calculations of the composition of two operators yields B_M. □

3.3 Recoverablity: a coercivity condition

Since $\phi \in \mathcal{H}_K$, ϕ is always a solution to the linear operator equation (52). However, this inverse problem may still be ill-posed. This happens when the solution is not unique or does not depend continuously on $\mathbf{f}_\phi$.

The uniqueness of the solution is not obvious. As explained above, we only observe an additive functional of ϕ induced by the structure of the governing equation:

$$\dot{\boldsymbol{x}}_i(t) = \sum_{i'=1}^{N} \phi(\|\boldsymbol{x}_{i'}(t) - \boldsymbol{x}_i(t)\|)(\boldsymbol{x}_{i'}(t) - \boldsymbol{x}_i(t)), \quad i = 1, \cdots, N. \tag{54}$$

Given $\boldsymbol{X}(t)$ and $\dot{\boldsymbol{X}}(t)$, one may attempt to solve the values of $\{\phi(\|\boldsymbol{x}_{i'}(t) - \boldsymbol{x}_i(t)\|)\}_{i,i'=1}^{N,N}$ from the constraints imposed by ODEs. However, we have dN equations but with only $\binom{N}{2}$ unknowns. In our numerical examples, $d = 1$ or 2, so as long as $N > 5$, the linear system is underdetermined. Even in the overdetermined case, there are no guarantees on the exact recovery of ϕ on the pairwise distances.

A coercivity condition To ensure the well-posedness, we require ϕ to be the unique solution to (52). So A has to be injective. Now we introduce a sufficient condition to guarantee the injectivity of the operator A. Using Lemma 8, $\mathcal{H}_K$ can be naturally embedded as a subspace of $L^2([0,R]; \tilde{\rho}_T^L \llcorner [0,R]; \mathbb{R})$.

Definition 12 (Coercivity condition)**.** *We say that the system* (4) *satisfies the* ***coercivity condition*** *on $\mathcal{H}_K$, if $\forall \varphi \in \mathcal{H}_K$, there exists $c_{\mathcal{H}_K} > 0$ such that*

$$\|A\varphi\|_{L^2(\rho_{\boldsymbol{X}})}^2 = \|\mathbf{f}_\varphi\|_{L^2(\rho_{\boldsymbol{X}})}^2 \geq c_{\mathcal{H}_K} \|\varphi\|_{L^2(\tilde{\rho}_T^L)}^2. \tag{55}$$

We choose the largest $c_{\mathcal{H}_K}$ that satisfies (55) *and refer to it as the coercivity constant.*

Then if $A\varphi = 0$ for $\varphi \in \mathcal{H}_K$, we conclude that $\varphi = 0$ everywhere on $[0,R]$ due to non-degeneracy of ρ_T^L on $[0,R]$ and the function φ is continuous. Therefore, A is injective. Below, we show the coercivity condition links our learning problem with a 1-dimensional kernel ridge regression problem in Problem 13: they are equivalent inverse problems.

Problem 13. *Consider learning $\phi \in \mathcal{H}_K$ from i.i.d noisy samples:*

$$y_m = \phi(r_m) + \epsilon_m, r_m \sim \tilde{\rho}_T^L, \epsilon_m \sim \mathcal{N}(0, \sigma^2), m = 1, \cdots, M. \tag{56}$$

One may want to find an estimator in the RKHS spanned by a Mercer kernel K. In the limiting case $M = \infty$, this learning problem can also be treated as an inverse problem, where one looks for the solution of the linear operator equation

$$J_{\tilde{\rho}_T^L}\varphi = \phi \tag{57}$$

and the operator $J_{\tilde{\rho}_T^L} : \mathcal{H}_K \to L^2([0,R]; \tilde{\rho}_T^L; \mathbb{R})$ is called the canonical inclusion map

$$J_{\tilde{\rho}_T^L}(\varphi)(r) = \langle \varphi, K_r \rangle_{\mathcal{H}_K}.$$

In general, this inverse problem is ill-posed, as ϕ may not be in the closure of $\mathrm{Im}(J_{\tilde{\rho}_T^L})$. One then looks for a solution to the least square problem

$$\arg\min_{\varphi \in \mathcal{H}_K} \|\varphi - \phi\|^2_{L^2(\tilde{\rho}_T^L)}. \tag{58}$$

Let P denote the projection mapping $L^2([0,R]; \tilde{\rho}_T^L; \mathbb{R})$ onto the closure of $\mathrm{Im}(J_{\tilde{\rho}_T^L})$. According to the theory of inverse problems, a sufficient condition for the existence and uniqueness of a minimal norm solution to the problem (58) is $P(\phi) \in \mathrm{Im}(J_{\tilde{\rho}_T^L})$. In fact, such a solution is exactly the Moore-Penrose (or generalized) solution to (58), denoted by $\phi^+_{\mathcal{H}_K}$, satisfying

$$J^*_{\tilde{\rho}_T^L} J_{\tilde{\rho}_T^L} \phi^+_{\mathcal{H}_K} = J^*_{\tilde{\rho}_T^L} \phi, \tag{59}$$

where the adjoint operator $J^*_{\tilde{\rho}_T^L}$ is an integral operator with respect to the kernel K, i.e., for $\varphi \in L^2([0,R]; \tilde{\rho}_T^L; \mathbb{R})$ and $r \in [0,R]$,

$$(J^*_{\tilde{\rho}_T^L}\varphi)(r) = \int_0^R K(r,r')\varphi(r') d\tilde{\rho}_T^L(r').$$

We know from the classical KRR learning theory (Smale and Zhou, 2007) that $J^*_{\tilde{\rho}_T^L} J_{\tilde{\rho}_T^L} : \mathcal{H}_K \to \mathcal{H}_K$ is a compact and positive operator, which ensured the well-posedness of (57). Below, we show A^*A is equivalent to $J^*_{\tilde{\rho}_T^L} J_{\tilde{\rho}_T^L}$ as an operator: their eigenvalues have the same asymptotic behaviours.

Proposition 14. *Let $\lambda_k^{\downarrow}(A^*A)$ and $\lambda_k^{\downarrow}(J^*_{\tilde{\rho}_T^L} J_{\tilde{\rho}_T^L})$ denote the k-th eigenvalue of A^*A and $J^*_{\tilde{\rho}_T^L} J_{\tilde{\rho}_T^L}$ respectively in decreasing order. If the coercivity condition* (55) *holds, then*

$$c_{\mathcal{H}_K} \lambda_k^{\downarrow}(J^*_{\tilde{\rho}_T^L} J_{\tilde{\rho}_T^L}) \le \lambda_k^{\downarrow}(A^*A) \le \lambda_k^{\downarrow}(J^*_{\tilde{\rho}_T^L} J_{\tilde{\rho}_T^L}).$$

Therefore, the coercivity condition bridges the study of our inverse problem with (57). To prove Proposition 14, we first show the following Proposition and Theorem.

Proposition 15. *The coercivity condition* (55) *implies that*

$$c_{\mathcal{H}_K} J^*_{\tilde{\rho}_T^L} J_{\tilde{\rho}_T^L} \le A^*A \le J^*_{\tilde{\rho}_T^L} J_{\tilde{\rho}_T^L}. \tag{60}$$

Proof. It suffices to show that, for any $\varphi \in \mathcal{H}_K$, we have that

$$c_{\mathcal{H}_K} \langle J^*_{\tilde{\rho}_T^L} J_{\tilde{\rho}_T^L} \varphi, \varphi \rangle_{\mathcal{H}_K} \le \langle A^*A\varphi, \varphi \rangle_{\mathcal{H}_K} \le \langle J^*_{\tilde{\rho}_T^L} J_{\tilde{\rho}_T^L} \varphi . \varphi \rangle_{\mathcal{H}_K}$$

The above inequality follows from the coercivity condition (55) and the identities

$$\langle J^*_{\tilde{\rho}_T^L} J_{\tilde{\rho}_T^L} \varphi, \varphi \rangle_{\mathcal{H}_K} = \|\varphi\|^2_{L^2(\tilde{\rho}_T^L)} \text{ and } \langle A^*A\varphi, \varphi \rangle_{\mathcal{H}_K} = \|A\varphi\|^2_{L^2(\rho_{\boldsymbol{X}})}. \tag{61}$$

□

Theorem 16 (Courant–Fischer–Weyl min-max principle, see (Bhatia, 2013)). *Let U be a compact, self-adjoint, positive operator on a Hilbert space $\mathcal{H}$, whose eigenvalues are listed in decreasing order $\lambda_1 \geq \lambda_2 \cdots$. Let $S_k \subset \mathcal{H}$ be a k-dimensional subspace. Then:*

$$\max_{S_k} \min_{x \in S_k, \|x\|=1} \langle Ux, x \rangle_{\mathcal{H}} = \lambda_k^{\downarrow}(U), \tag{62}$$

$$\min_{S_{k-1}} \max_{x \in S_{k-1}^{\perp}, \|x\|=1} \langle Ux, x \rangle_{\mathcal{H}} = \lambda_k^{\downarrow}(U). \tag{63}$$

Now we are ready to present the proof.

Proof of Proposition 14. Let $\lambda_k^{\downarrow}(A^*A)$ denote the kth eigenvalue of A^*A in decreasing order. First, we recall that for two positive operators A_1 and A_2 on $\mathcal{H}$, $A_1 \leq A_2$ means that $\langle A_1 x, x \rangle_{\mathcal{H}} \leq \langle A_2 x, x \rangle_{\mathcal{H}}$ for all $x \in \mathcal{H}$. The inequality (60) in Proposition 15 together with the equality (62) yield that

$$\begin{aligned} c_{\mathcal{H}_K} \lambda_k^{\downarrow}(J_{\tilde{\rho}_T^L}^* J_{\tilde{\rho}_T^L}) = \max_{S_k} \min_{x \in S_k, \|x\|=1} \langle c_{\mathcal{H}_K} J_{\tilde{\rho}_T^L}^* J_{\tilde{\rho}_T^L} x, x \rangle_{\mathcal{H}_K} &\leq \lambda_k^{\downarrow}(A^*A) = \max_{S_k} \min_{x \in S_k, \|x\|=1} \langle A^*Ax, x \rangle_{\mathcal{H}_K} \\ &\leq \max_{S_k} \min_{x \in S_k, \|x\|=1} \langle J_{\tilde{\rho}_T^L}^* J_{\tilde{\rho}_T^L} x, x \rangle_{\mathcal{H}} \\ &= \lambda_k^{\downarrow}(J_{\tilde{\rho}_T^L}^* J_{\tilde{\rho}_T^L}). \end{aligned}$$

Therefore,

$$c_{\mathcal{H}_K} \lambda_k^{\downarrow}(J_{\tilde{\rho}_T^L}^* J_{\tilde{\rho}_T^L}) \leq \lambda_k^{\downarrow}(A^*A) \leq \lambda_k^{\downarrow}(J_{\tilde{\rho}_T^L}^* J_{\tilde{\rho}_T^L}).$$

□

Since the coercivity condition implies the injectivity of A, ϕ is the unique generalized solution to the equation

$$A^*A\phi^+ = A^*\mathbf{f}_\phi.$$

However, this generalized solution may not depend continuously on the datum $\mathbf{f}_\phi$, so that finding ϕ is again an ill-posed problem when the datum $\mathbf{f}_\phi$ is contaminated by noise. In the literature of the inverse problem, one way to overcome this issue is to introduce the Tikhonov regularization technique and consider a risk functional with a possible regularization term determined by $\lambda \geq 0$:

$$\mathcal{E}^{\lambda,\infty}(\varphi) := \|A\varphi - \mathbf{f}_\phi\|_{L^2(\rho_{\boldsymbol{X}})}^2 + \lambda \|\varphi\|_{\mathcal{H}_K}^2. \tag{64}$$

When the data is finite and noisy, it is impossible to achieve the exact recovery of ϕ. Similar to the case of infinite data, one may consider solving

$$\phi_{\mathcal{H}_K}^{\lambda,M} := \arg\min_{\varphi \in \mathcal{H}_K} \mathcal{E}^{\lambda,M}(\varphi) \tag{65}$$

$$\mathcal{E}^{\lambda,M}(\varphi) := \|A_M\varphi - \mathbb{V}_{\sigma^2,M}\|^2 + \lambda \|\varphi\|_{\mathcal{H}_K}^2 \tag{66}$$

(66) provides an alternative approach to learn ϕ from data. When A is the identity, (65) is called the KRR estimator. In classical nonparametric regression problems such as Problem 13, one can also model ϕ as a GP with a suitable prior and then approximate ϕ by the posterior mean estimator. There is a well-known connection between the posterior mean estimator of the GP approach with the KRR estimator. In our paper, we shall generalize this classical fact to our setting: we show that the posterior mean estimator (8) with a suitable prior coincides with $\phi_{\mathcal{H}_K}^{\lambda,M}$.

The connection between our posterior mean estimator with $\phi_{\mathcal{H}_K}^{\lambda,M}$ allows us to use the operator algebra framework to derive quantitative error analysis for our approach, since $\phi_{\mathcal{H}_K}^{\lambda,M}$ admits an operator representation.

Proposition 17. *Consider the expected risk $\mathcal{E}^{\lambda,\infty}(\cdot)$ in (64) as well as its empirical version $\mathcal{E}^{\lambda,M}(\cdot)$ in (65). Let $\phi^{\lambda,\infty}_{\mathcal{H}_K}$ and $\phi^{\lambda,M}_{\mathcal{H}_K}$ be their minimizers respectively.*

- *Case $\lambda = 0$. The minimizer $\phi^{0,\infty}_{\mathcal{H}_K}$ always exists and satisfies*

$$B\phi^{0,\infty}_{\mathcal{H}_K} = A^*\mathbf{f}_\phi, B = A^*A.$$

- *Case $\lambda > 0$. Then $\phi^{\lambda,\infty}_{\mathcal{H}_K}$ and $\phi^{\lambda,M}_{\mathcal{H}_K}$ are unique minimizers and they are given by*

$$\phi^{\lambda,\infty}_{\mathcal{H}_K} := (B+\lambda)^{-1}A^*\mathbf{f}_\phi. \tag{67}$$
$$\phi^{\lambda,M}_{\mathcal{H}_K} := (B_M+\lambda)^{-1}A_M^*\mathbb{V}_{\sigma^2,M}, B_M = A_M^*A_M. \tag{68}$$

The proof of this Proposition follows from solving the norm equation of the corresponding regularized least squares.

Below, we derive a Representer theorem for $\phi^{\lambda,M}_{\mathcal{H}_K}$, which is key to establish the connection. It shows that $\phi^{\lambda,M}_{\mathcal{H}_K}$ is, in fact, a linear combination of the kernel function K_r, where r ranges in pairwise distances of agents coming from the observational data.

Theorem 18 (Representer theorem)**.** *If $\lambda > 0$, the minimizer of the regularized empirical risk functional $\mathcal{E}^{\lambda,M}(\cdot)$ (see (66)) has the form*

$$\phi^{\lambda,M}_{\mathcal{H}_K} = \sum_{r\in r_{\mathbb{X}_M}} \hat{c}_r K_r, \tag{69}$$

where $r_{\mathbb{X}_M} \in \mathbb{R}^{MLN^2}$ is the set which contains all the pairwise distances in $\mathbb{X}_M$, i.e.

$$r_{\mathbb{X}_M} = \left[r_{11}^{(1,1)},\dots,r_{1N}^{(1,1)},\dots,r_{N1}^{(1,1)},\dots,r_{NN}^{(1,1)},\dots,r_{11}^{(M,L)},\dots,r_{1N}^{(M,L)},\dots,r_{N1}^{(M,L)},\dots,r_{NN}^{(M,L)}\right]^T. \tag{70}$$

Moreover, denote by $\hat{\mathbf{c}}$ the vectorization of $\hat{c}_r$ for r in $r_{\mathbb{X}_M}$, we have that

$$\hat{\mathbf{c}} = \frac{1}{N}\boldsymbol{r}_{\mathbb{X}_M}^T \cdot (K_{\mathbf{f}_\phi}(\mathbb{X}_M,\mathbb{X}_M) + \lambda NMLI)^{-1}\mathbb{V}_{\sigma^2,M}, \tag{71}$$

where the block-diagonal matrix $\boldsymbol{r}_{\mathbb{X}_M} = \mathrm{diag}(\boldsymbol{r}_{\boldsymbol{X}^{(m,l)}}) \in \mathbb{R}^{MLdN\times MLN^2}$ and $\boldsymbol{r}_{\boldsymbol{X}^{(m,l)}} \in \mathbb{R}^{dN\times N^2}$ defined by

$$\boldsymbol{r}_{\boldsymbol{X}^{(m,l)}} = \begin{bmatrix} \boldsymbol{r}_{11}^{(m,l)},\dots,\boldsymbol{r}_{1N}^{(m,l)} & \mathbf{0} & \cdots & \mathbf{0} \\ \mathbf{0} & \boldsymbol{r}_{21}^{(m,l)},\dots,\boldsymbol{r}_{2N}^{(m,l)} & \cdots & \mathbf{0} \\ \vdots & \vdots & \ddots & \vdots \\ \mathbf{0} & \mathbf{0} & \cdots & \boldsymbol{r}_{N1}^{(m,l)},\dots,\boldsymbol{r}_{NN}^{(m,l)} \end{bmatrix}. \tag{72}$$

Proof of Theorem 18. The proof is based on the operator representations of minimizers which allow us to use tools from the spectral theory of operator algebra.

Let $\mathcal{H}_{K,M}$ be the subspace of $\mathcal{H}_K$ spanned by the set of functions $\{K_r : r \in r_{\mathbb{X}_M}\}$. By Proposition 11, we know that $B_M(\mathcal{H}_{K,M}) \subset \mathcal{H}_{K,M}$. Since B_M is self-adjoint and compact, by the spectral theory of self-adjoint compact operators (see (Blank et al., 2008)), $\mathcal{H}_{K,M}$ is also an invariant subspace for the operator $(B_M+\lambda I)^{-1}$. Then by (68), there exists a vector $\hat{c}$ such that

$$\phi^{\lambda,M}_{\mathcal{H}} = \sum_{r\in r_{\mathbb{X}_M}} \hat{c}_r K_r. \tag{73}$$

Then, multiplying $(B_M + \lambda I)$ on both sides of (68) and plugging (73) into the identity, we can obtain

$$\big(\boldsymbol{r}_{\mathbb{X}_M}^T \boldsymbol{r}_{\mathbb{X}_M} K(r_{\mathbb{X}_M}, r_{\mathbb{X}_M}) + \lambda N^3 MLI\big)\hat{\mathbf{c}} = N\boldsymbol{r}_{\mathbb{X}_M}^T \mathbb{V}_{\sigma^2,M}, \tag{74}$$

where we used the matrix representation of $(B_M + \lambda I)$ with respect to the spanning set $\{K_r : r \in r_{\mathbb{X}_M}\}$.

Recall that we have $K(r_{\mathbb{X}_M}, r_{\mathbb{X}_M}) = (K(r_{ij}, r_{i'j'}))_{r_{ij}, r_{i'j'} \in r_{\mathbb{X}_M}}$ and $K_{\mathbf{f}_\phi}(\mathbb{X}_M, \mathbb{X}_M) = \mathrm{Cov}(\mathbf{f}_\phi(\mathbb{X}_M), \mathbf{f}_\phi(\mathbb{X}_M))$. By the identity

$$\boldsymbol{r}_{\mathbb{X}_M} K(r_{\mathbb{X}_M}, r_{\mathbb{X}_M}) \boldsymbol{r}_{\mathbb{X}_M}^T = N^2 K_{\mathbf{f}_\phi}(\mathbb{X}_M, \mathbb{X}_M) \tag{75}$$

and the fact that the matrix in the left hand side of (74) is invertible, one can verify that

$$\hat{\mathbf{c}} = \frac{1}{N}\boldsymbol{r}_{\mathbb{X}_M}^T \cdot (K_{\mathbf{f}_\phi}(\mathbb{X}_M, \mathbb{X}_M) + \lambda NMLI)^{-1} \mathbb{V}_{\sigma^2,M} \tag{76}$$

is the solution. □

3.4 Operator representations of posterior mean estimators and marginal variances

Leveraging Theorem 18, we derive operator representations for posterior mean estimators and marginal variances. Note that this result does not require the coercivity condition.

Theorem 19. *Suppose $\phi \sim \mathcal{GP}(0, \tilde{K})$ with $\tilde{K} = \frac{\sigma^2 K}{MNL\lambda}$ for some $\lambda > 0$.*

- *The posterior mean estimator $\bar{\phi}_M$ in (8) has an operator representation*

$$\bar{\phi}_M := (A_M^* A_M + \lambda)^{-1} A_M^* \mathbb{V}_{\sigma^2,M} \tag{77}$$

- *The marginal posterior variance (9) can be written as*

$$\mathrm{Var}(\phi_M(r_*)|\mathbb{Y}_{\sigma^2,M}) = \frac{\sigma^2}{ML\lambda N}[K_{r_*}(r_*) - K_{r_*}^{\lambda,M}(r_*)], \tag{78}$$

  where the function $K_{r_*}(\cdot) := K(r_*, \cdot)$, and $K_{r_*}^{\lambda,M} := (A_M^* A_M + \lambda)^{-1} A_M^* \mathbf{f}_{K_{r_*}}(\mathbb{X}_M)$.

Proof of Theorem 19. Let $\tilde{K} = \frac{\sigma^2 K}{MNL\lambda}$.

- Since $\phi \sim \mathcal{GP}(0, \tilde{K})$, the posterior mean estimator (8) becomes

$$\begin{aligned}
\bar{\phi}_M(r^*) &= \tilde{K}_{\phi,\mathbf{f}_\phi}(r^*, \mathbb{X}_M)(\tilde{K}_{\mathbf{f}_\phi}(\mathbb{X}_M, \mathbb{X}_M) + \sigma^2 I)^{-1} \mathbb{V}_{\sigma^2,M} \\
&= \frac{1}{N}\tilde{K}_{r_{\mathbb{X}_M}^T}(r^*) \boldsymbol{r}_{\mathbb{X}_M}^T (\tilde{K}_{\mathbf{f}_\phi}(\mathbb{X}_M, \mathbb{X}_M) + \sigma^2 I)^{-1} \mathbb{V}_{\sigma^2,M} \\
&= \frac{1}{N} K_{r_{\mathbb{X}_M}^T}(r^*) \boldsymbol{r}_{\mathbb{X}_M}^T (K_{\mathbf{f}_\phi}(\mathbb{X}_M, \mathbb{X}_M) + NMLI)^{-1} \mathbb{V}_{\sigma^2,M} \\
&= K_{\phi,\mathbf{f}_\phi}(r^*, \mathbb{X}_M)(K_{\mathbf{f}_\phi}(\mathbb{X}_M, \mathbb{X}_M) + NMLI)^{-1} \mathbb{V}_{\sigma^2,M} \\
&= \sum_{r \in r_{\mathbb{X}_M}} \hat{c}_r K_r,
\end{aligned}$$

  where $\hat{c}$ is defined in (71) and we use the identity $K_{\phi,\mathbf{f}_\phi}(r^*, \mathbb{X}_M) = \frac{1}{N} K_{r_{\mathbb{X}_M}^T}(r^*) \boldsymbol{r}_{\mathbb{X}_M}^T$ (also for $\tilde{K}$) in the proof.

- We replace the regression target ϕ with the function K_{r^*}, and use the same analysis to develop a representer theorem similar to (18) for the empirical regularized risk functional (66). Specifically, we have that

$$K_{r_*}^{\lambda,M}(\cdot) = K_{\phi,\mathbf{f}_\phi}(\cdot,\mathbb{X}_M)(K_{\mathbf{f}_\phi}(\mathbb{X}_M,\mathbb{X}_M) + ML\lambda NI)^{-1}K_{\mathbf{f}_\phi,\phi}(\mathbb{X}_M,r^*).$$

Since $\phi \sim \mathcal{GP}(0,\tilde{K})$, the marginal posterior variance in (9) will then become

$$\begin{aligned}
&\mathrm{Var}(\phi_M(r_*)|\mathbb{Y}_{\sigma^2,M}) \\
&= \tilde{K}_{r^*}(r^*) - \tilde{K}_{\phi,\mathbf{f}_\phi}(r^*,\mathbb{X}_M)(\tilde{K}_{\mathbf{f}_\phi}(\mathbb{X}_M,\mathbb{X}_M) + \sigma^2 I)^{-1}\tilde{K}_{\mathbf{f}_\phi,\phi}(\mathbb{X}_M,r^*) \\
&= \frac{\sigma^2}{ML\lambda N}\left(K_{r^*}(r^*) - K_{\phi,\mathbf{f}_\phi}(r^*,\mathbb{X}_M)(\frac{\sigma^2}{ML\lambda N}K_{\mathbf{f}_\phi}(\mathbb{X}_M,\mathbb{X}_M) + \sigma^2 I)^{-1}\frac{\sigma^2}{ML\lambda N}K_{\mathbf{f}_\phi,\phi}(\mathbb{X}_M,r^*)\right) \\
&= \frac{\sigma^2}{ML\lambda N}[K(r^*,r^*) - K_{r_*}^{\lambda,M}(r^*)]
\end{aligned}$$

□

Applying Theorem 19, the analysis of reconstruction error for our posterior mean estimator and marginal posterior variance can be performed equivalently on $\phi_{\mathcal{H}_K}^{\lambda,M}$ and $K_{r_*}(r_*) - K_{r_*}^{\lambda,M}(r_*)$. We shall next develop estimates of the error $\phi_{\mathcal{H}_K}^{\lambda,M} - \phi$ and the marginal posterior variance can be analyzed similarly by replacing ϕ with K_{r^*}.

3.5 Finite sample analysis of errors

In nonparametric regression and inverse problems, one of the fundamental problems to address is the convergence of estimators obtained from finite data. Without constraints on the target function, we can always find a solution with convergence guarantees but the convergence rates can be arbitrarily slow. This is called the "no free lunch theorem" in learning theory (Devroye et al., 2013) and a similar kind of phenomenon occurs in the regularization of ill-posed inverse problems (Engle and Neubauer, 1996).

Source condition In solving Problem 13, a standard way to impose restrictions on target functions is to describe a prior on ϕ determined by smoothness conditions. One typically assumes (Smale and Zhou, 2007)

$$\phi \in \tilde{\Omega}_{\alpha,S} = \{\varphi \in L^2(\tilde{\rho}_T^L) : \varphi = (J_{\tilde{\rho}_T^L}J_{\tilde{\rho}_T^L}^*)^\alpha\psi, \|\psi\|_{L^2(\tilde{\rho}_T^L)} \le S\}, \tag{79}$$

and α typically ranges from 0 to 1. When $\alpha = 0$, this condition is equivalent to $\phi \in L^2(\tilde{\rho}_T^L)$; as α increases, ϕ becomes more smooth. For example, we have $\phi \in \mathcal{H}_K$ as long as $\alpha \ge \frac{1}{2}$. The value S measures the complexity of φ. A function φ with many oscillations will force S to be large.

As noted (De Vito et al., 2005; Caponnetto and De Vito, 2005), (79) corresponds to what is called source conditions in the context of solving linear inverse problems (57). When $\phi \in \tilde{\Omega}_{\alpha,S}$ with $\alpha > \frac{1}{2}$, it is equivalent to consider the Hölder type source condition

$$\phi \in \Omega_{\gamma,S} = \{\varphi \in \mathcal{H}_K : \varphi = (J_{\tilde{\rho}_T^L}^*J_{\tilde{\rho}_T^L})^\gamma\psi, \|\psi\|_{\mathcal{H}_K}^2 \le S\},$$

where $\gamma = \alpha - \frac{1}{2}$. One can refer to section 2.3 of (Bauer et al., 2007) for more details. Following inverse problem literature and the connection between $(J_{\tilde{\rho}_T^L}^*J_{\tilde{\rho}_T^L})$ and A^*A established in Proposition 14, we shall consider the standard Hölder type source condition for our inverse problem.

Assumption 20. *$\phi \in \mathrm{Im}(B^\gamma)$ with $\gamma \in (0,\frac{1}{2}]$, where $B = A^*A$.*

3.5.1 Decomposition of the reconstruction error

Using the operator representations, we perform the decomposition of the reconstruction error as the sum of two types of errors:

$$\begin{aligned}\phi_{\mathcal{H}_K}^{\lambda,M} - \phi &= \phi_{\mathcal{H}_K}^{\lambda,M} - \phi_{\mathcal{H}_K}^{\lambda,\infty} + \phi_{\mathcal{H}_K}^{\lambda,\infty} - \phi \\ &= \underbrace{(B_M+\lambda)^{-1}A_M^*\mathbb{V}_{\sigma^2,M} - (B+\lambda)^{-1}A^*\mathbf{f}_\phi}_{\text{Sample error}} + \underbrace{(B+\lambda)^{-1}A^*\mathbf{f}_\phi - \phi}_{\text{Approximation error}}.\end{aligned}$$

The sample error comes from two sources: one is from the randomness in the initial conditions of observed trajectories, and the second one is the randomness in the noise term. We further decouple the sample error into the noise part and noise-free part; we have that:

$$\begin{aligned}\phi_{\mathcal{H}_K}^{\lambda,M} - \phi_{\mathcal{H}_K}^{\lambda,\infty} &= (B_M+\lambda)^{-1}A_M^*\mathbb{V}_{\sigma^2,M} - \phi_{\mathcal{H}_K}^{\lambda,\infty} \\ &= \underbrace{(B_M+\lambda)^{-1}B_M\phi - (B+\lambda)^{-1}B\phi}_{\tilde{\phi}_{\mathcal{H}_K}^{\lambda,M} - \phi_{\mathcal{H}_K}^{\lambda,\infty}} + \underbrace{(B_M+\lambda)^{-1}A_M^*\mathbb{W}_M}_{\text{Noise term}}\end{aligned}$$

where $\tilde{\phi}_{\mathcal{H}_K}^{\lambda,M}$ is the empirical minimizer of $\mathcal{E}^{\lambda,M}(\cdot)$ for noise-free observations and $\mathbb{W}_M$ denotes the noise vector.

One of our key technical contributions is to provide a detailed analysis of the operators A ($B = A^*A$) and A_M ($B_M = A_M^*A_M$), and prove the concentration inequalities for operators.

Analysis of sample error $\|\phi_{\mathcal{H}_K}^{\lambda,M} - \phi_{\mathcal{H}_K}^{\lambda,\infty}\|_{\mathcal{H}_K}$. We first provide non-asymptotic analysis of the sample error

$$\|(B_M+\lambda)^{-1}B_M\varphi - (B+\lambda)^{-1}B\varphi\|_{\mathcal{H}_K}$$

for any $\varphi \in \mathcal{H}_K$. Then we apply the bound to ϕ and obtain an error estimate of $\|\tilde{\phi}_{\mathcal{H}_K}^{\lambda,M} - \phi_{\mathcal{H}_K}^{\lambda,M}\|_{\mathcal{H}_K}$. We shall need the following lemmas.

Lemma 21. *For any bounded function $\varphi \in L^2(\tilde{\rho}_T^L)$ and any positive integer M, we have that*

$$\|B_M\varphi\|_{\mathcal{H}_K} \leq \kappa R^2\|\varphi\|_\infty, a.s., \tag{80}$$

$$\mathbb{E}\|B_M\varphi\|_{\mathcal{H}_K}^2 \leq \|\varphi\|_{L^2(\tilde{\rho}_T^L)}^2\kappa^2R^2. \tag{81}$$

Lemma 22. *For a bounded function $\varphi \in L^2(\tilde{\rho}_T^L)$ and $0 < \delta < 1$, with probability at least $1-\delta$, there holds*

$$\|B_M\varphi - B\varphi\|_{\mathcal{H}_K} \leq \frac{4\kappa R^2\|\varphi\|_\infty\log(2/\delta)}{M} + \kappa R\|\varphi\|_{L^2(\tilde{\rho}_T^L)}\sqrt{\frac{2\log(2/\delta)}{M}}. \tag{82}$$

Lemma 23. *For a bounded function $\varphi \in L^2(\tilde{\rho}_T^L)$ and $0 < \delta < 1$, with probability at least $1-\delta$, there holds*

$$\|(B_M+\lambda)^{-1}B_M\varphi - (B+\lambda)^{-1}B\varphi\|_{\mathcal{H}_K} \leq \frac{\kappa R^2\|\varphi\|_\infty\sqrt{2\log(4/\delta)}}{\sqrt{M}\lambda}\left(C_{\kappa,\mathcal{H}_K} + \frac{C_{\kappa,R,\lambda}\sqrt{2\log(4/\delta)}}{\sqrt{M\lambda}}\right),$$

where $C_{\kappa,\mathcal{H}_K} = (\kappa+1)\sqrt{\frac{2}{c_{\mathcal{H}_K}}}$ and $C_{\kappa,R,\lambda} = \kappa R + \sqrt{\lambda}$.

Finally, we can analyze the perturbation $(B_M+\lambda)^{-1}A_M^*\mathbb{W}_M$ caused by the noise and obtain a bound for the sample error.

Theorem 24 (Sample error bound). *For any $\delta \in (0,1)$, it holds with probability at least $1-\delta$ that*

$$\|\phi_{\mathcal{H}_K}^{\lambda,M} - \phi_{\mathcal{H}_K}^{\lambda,\infty}\|_{\mathcal{H}_K} \lesssim \frac{\kappa R^2 \|\phi\|_\infty \sqrt{2\log(8/\delta)}}{\sqrt{M}\lambda} \left(C_{\kappa,\mathcal{H}_K} + \frac{C_{\kappa,R,\lambda}\sqrt{2\log(8/\delta)}}{\sqrt{M\lambda}} \right) + \frac{2\kappa R\sigma \log(8/\delta)}{\sqrt{c}\lambda d\sqrt{MLN}},$$

where c is an absolute constant appearing in the Hanson-Wright inequality (Theorem 30), $C_{\kappa,\mathcal{H}_K} = (\kappa+1)\sqrt{\frac{2}{c_{\mathcal{H}_K}}}$ and $C_{\kappa,R,\lambda} = \kappa R + \sqrt{\lambda}$.

The detailed proofs of the above lemmas and theorem are shown in Appendix A.

Analysis of approximation error $\|\phi_{\mathcal{H}_K}^{\lambda,\infty} - \phi\|_{\mathcal{H}_K}$. Under the standard source condition (Assumption 20), the analysis of $\|\phi_{\mathcal{H}_K}^{\lambda,\infty} - \phi\|_{\mathcal{H}_K}$ follows the routine in the literature of Tikhonov regularization (see section 5 in (Caponnetto and De Vito, 2005)). For the sake of being self-contained, we still present the analysis here.

Recall that $B = A^*A$ is a positive compact operator. Let $B = \sum_{n=1}^N \lambda_n \langle \cdot, e_n\rangle e_n$ (possibly $N=\infty$) be the spectral decomposition of B with $0 < \lambda_{n+1} < \lambda_n$ and $\{e_n\}_{n=1}^N$ be an orthonormal basis of $\mathcal{H}_K$. Then

$$\begin{aligned}
\|\phi_{\mathcal{H}_K}^{\lambda,\infty} - \phi\|_{\mathcal{H}_K}^2 &= \|(B+\lambda)^{-1}B\phi - \phi\|_{\mathcal{H}_K}^2 \\
&= \|\lambda(B+\lambda)^{-1}\phi\|_{\mathcal{H}_K}^2 \\
&= \sum_{n=1}^N \left(\frac{\lambda}{\lambda_n+\lambda}\right)^2 |\langle \phi, e_n\rangle_{\mathcal{H}_K}|^2. \qquad (83)
\end{aligned}$$

Assume now that $\phi \in \mathrm{Im}(B^\gamma)$ with $0 < \gamma \le \frac{1}{2}$. Since the function x^γ is concave on $[0,\infty]$, $\frac{\lambda}{\lambda_n+\lambda} \le \frac{\lambda^\gamma}{\lambda_n^\gamma}$. Then we have $\|\phi_{\mathcal{H}_K}^{\lambda,\infty} - \phi\|_{\mathcal{H}_K} \le \lambda^\gamma \|B^{-\gamma}\phi\|_{\mathcal{H}_K}$ where $B^{-\gamma}\phi$ represents the pre-image of ϕ.

Theorem 25 (Convergence rate for posterior mean estimator). *Suppose that $\phi \in \mathrm{Im}(B^\gamma)$ for some $\gamma \in (0, \frac{1}{2}]$. If we choose $\lambda \asymp M^{-\frac{1}{2\gamma+2}}$, then for any $\delta \in (0,1)$, it holds with probability at least $1-\delta$ that*

$$\|\phi_{\mathcal{H}_K}^{\lambda,M} - \phi\|_{\mathcal{H}_K} \lesssim C(\phi,\kappa,R,c_{\mathcal{H}_K},\sigma)\log(\frac{8}{\delta})M^{-\frac{\gamma}{2\gamma+2}},$$

where $C = \max\{\frac{\kappa R^2\|\phi\|_\infty}{\sqrt{c_{\mathcal{H}_K}}}, \frac{2\kappa R\sigma}{\sqrt{LN}d}, \|g\|_{\mathcal{H}_K}\}$, with g satisfying $(A^*A)^\gamma(g) = \phi$.

Proof. Without loss of generality, let $\lambda = M^{-\frac{1}{2\gamma+2}}$. By Theorem 24 and approximation error (83), with a probability at least $1-\delta$, we have that

$$\begin{aligned}
&\|\phi_{\mathcal{H}_K}^{\lambda,M} - \phi\|_{\mathcal{H}_K} \le \|\phi_{\mathcal{H}_K}^{\lambda,M} - \phi_{\mathcal{H}_K}^{\lambda,\infty}\|_{\mathcal{H}_K} + \|\phi_{\mathcal{H}_K}^{\lambda,\infty} - \phi\|_{\mathcal{H}_K} \\
\le& \frac{\kappa R^2\|\phi\|_\infty\sqrt{2\log(8/\delta)}}{\sqrt{M}\lambda}\left(C_{\kappa,\mathcal{H}_K} + \frac{C_{\kappa,R,\lambda}\sqrt{2\log(8/\delta)}}{\sqrt{M\lambda}}\right) + \frac{2\kappa R\sigma\log(8/\delta)}{\sqrt{c}\lambda d\sqrt{MLN}} + \lambda^\gamma\|B^{-\gamma}\phi\|_{\mathcal{H}_K} \\
\lesssim& C_1 M^{-\frac{\gamma}{2\gamma+2}}\sqrt{\log(8/\delta)} + C_2 M^{-\frac{\gamma}{2\gamma+2}} M^{-\frac{1+2\gamma}{4+4\gamma}}\log(8/\delta) + C_3 M^{-\frac{\gamma}{2\gamma+2}} \\
\le& C\log(\frac{8}{\delta})M^{-\frac{\gamma}{2\gamma+2}},
\end{aligned}$$

where $C = \max\{\frac{\kappa^2R^2\|\phi\|_\infty}{\sqrt{c_{\mathcal{H}_K}}}, \frac{2\kappa R\sigma}{\sqrt{cLN}d}, \|B^{-\gamma}\phi\|_{\mathcal{H}_K}\}$, and the symbol $\lesssim$ means that the inequality holds up to a multiplicative constant that is independent of the listed parameters. □

Finally, we provide an L^∞ error analysis for marginal posterior variance (9).

Theorem 26. *For any $\delta \in (0,1)$, it holds with probability at least $1-\delta$ that*

$$|\mathrm{Var}(\bar{\phi}(r_*)|\mathbb{Y}_M)| \leq \frac{\kappa\sigma^2}{ML\lambda N}\left(\kappa + \frac{\kappa R^2\|K_{r^*}\|_\infty\sqrt{2\log(4/\delta)}}{\sqrt{M\lambda}}\left(C_{\kappa,\mathcal{H}_K} + \frac{C_{\kappa,R,\lambda}\sqrt{2\log(4/\delta)}}{\sqrt{M\lambda}}\right)\right),$$

where $C_{\kappa,\mathcal{H}_K} = (\kappa+1)\sqrt{\frac{2}{c_{\mathcal{H}_K}}}$ and $C_{\kappa,R,\lambda} = \kappa R + \sqrt{\lambda}$.

Proof. Note that $K_{r^*}^{\lambda,M} = (B_M+\lambda)^{-1}B_M K_{r^*}$. Then

$$\begin{aligned} K_{r^*}^{\lambda,M} - K_{r^*} &= (B_M+\lambda)^{-1}B_M K_{r^*} - (B+\lambda)^{-1}BK_{r^*} + (B+\lambda)^{-1}BK_{r^*} - K_{r^*} \\ &= (B_M+\lambda)^{-1}B_M K_{r^*} - (B+\lambda)^{-1}BK_{r^*} + \lambda(B+\lambda)^{-1}K_{r^*}. \end{aligned}$$

Applying Theorem 23 to K_{r^*}, we know that, for any $0<\delta<1$, with probability at least $1-\delta$, there holds

$$\|(B_M+\lambda)^{-1}B_M K_{r^*} - (B+\lambda)^{-1}BK_{r^*}\|_{\mathcal{H}_K} \leq \frac{\kappa R^2\|K_{r^*}\|_\infty\sqrt{2\log(4/\delta)}}{\sqrt{M\lambda}}\left(C_{\kappa,\mathcal{H}_K} + \frac{C_{\kappa,R,\lambda}\sqrt{2\log(4/\delta)}}{\sqrt{M\lambda}}\right).$$

On the other hand,

$$\|\lambda(B+\lambda)^{-1}K_{r^*}\|_{\mathcal{H}_K} \leq \|K_{r^*}\|_{\mathcal{H}_K}.$$

Therefore, for any $0<\delta<1$, with probability at least $1-\delta$,

$$\begin{aligned} |\mathrm{Var}(\bar{\phi}(r_*)|\mathbb{Y}_M)| &\leq \frac{\sigma^2}{ML\lambda N}\|K_{r^*}^{\lambda,M} - K_{r^*}\|_\infty \\ &\leq \frac{\kappa\sigma^2}{ML\lambda N}\|K_{r^*}^{\lambda,M} - K_{r^*}\|_{\mathcal{H}_K} \\ &\leq \frac{\kappa\sigma^2}{ML\lambda N}\left(\kappa + \frac{\kappa R^2\|K_{r^*}\|_\infty\sqrt{2\log(4/\delta)}}{\sqrt{M\lambda}}\left(C_{\kappa,\mathcal{H}_K} + \frac{C_{\kappa,R,\lambda}\sqrt{2\log(4/\delta)}}{\sqrt{M\lambda}}\right)\right). \end{aligned}$$

The conclusion follows.

□

Discussions

- The coercivity constant $c_{\mathcal{H}_K}$ in fact depends on N, L, μ_0 and $\mathcal{H}_K$. In our paper, we consider both N and L fixed. We can prove that $c_{\mathcal{H}_K} \geq \frac{N-1}{N^2}$ and can even be independent of N for the case of $L=1$ for certain initial distributions (see section 3.6). If L changes, the measure $\tilde{\rho}_T^L$ will also change. It is not clear if $c_{\mathcal{H}_K}$ would increase as L increases. We defer more detailed discussions to section 3.6. In addition, our theoretical framework suggests that it is possible to use a part of equations ($N_1 << N$) for learning, as long as a form of coercivity condition is satisfied. We leave it for future investigation.

- We show that a parametric learning rate in terms of M for marginal posterior variance can be obtained. In particular, from our analysis of the coercivity condition, it is possible to show the bound is proportional to $\frac{1}{N}$ (number of particles) for the case of $L=1$, when $c_{\mathcal{H}_K}$ is independent of N (see an example in section 3.6) due to the independence of noise. For higher $L>1$, the dependence of $c_{\mathcal{H}_K}$ on N is unclear. For the reconstruction error, the current rate only sees M as the effective sample size, i.e. number of random samples. Obtaining this rate is satisfactory because we do not observe the values of ϕ and the pairwise distances are in general correlated. The convergence rate in M coincides with

the optimal minimax rate achieved in the classical 1-dimensional KRR problem, Problem 13, for the set of functions $\Omega_{\gamma,S}$, see the summary in the second column of Table 1 in (Blanchard and Mücke, 2018) and their associated references. Our convergence rate is done for all Mercer kernels, where one can refer to $s = 0$ (reconstruction error) and $b \to 1^+$ in the main result of (Blanchard and Mücke, 2018). Using our framework as the bridge, we believe we can obtain more refined rates and bounds if we know, for example, the decay of eigenvalues of A. This opens many future questions to investigate.

- Recall in Remark 2, if $K \in C^{2s+\epsilon}([0,R]\times[0,R])$ with $0 < \epsilon < 2$, we have $\|\varphi\|_{C^s} \leq 4^s \|K\|_{C^{2s}}^{\frac{1}{2}} \|\varphi\|_{\mathcal{H}_K}, \forall \varphi \in \mathcal{H}_K$. Therefore, we obtain the convergence rate in terms of C^s norm, which is a stronger norm than the previous L^2 convergence (Lu et al., 2019).

3.6 Discussion on the coercivity constant

The coercivity condition was proposed in (Lu et al., 2019), where a least square approach was proposed to learn ϕ over a suitably chosen hypothesis function space with complexity adaptive to data. The coercivity condition (55) in this paper can be viewed as a special instance when the hypothesis space is set to be $\mathcal{H}_K$. We review below briefly the recent study on the coercivity condition.

When the initial distributions of the agents are exchangeable, the coercivity condition is closely related to the positiveness of integral operators that arise in (55):

$$\begin{aligned}\kappa_{\mathcal{H}_K}\|\varphi\|^2_{L^2(\tilde{\rho}_T^L)} &\leq \frac{1}{L}\sum_{l=1}^{L}\mathbb{E}_{\boldsymbol{X}(0)\sim\mu_0}[\varphi(|\boldsymbol{r}_{12}(t_l)|)\varphi(|\boldsymbol{r}_{13}(t_l)|)\langle \boldsymbol{r}_{12}(t_l),\boldsymbol{r}_{13}(t_l)\rangle] \\ &= \int_0^\infty\int_0^\infty \varphi(r)\varphi(s)\overline{K}(r,s)drds, \forall \varphi\in\mathcal{H}_K\end{aligned}$$

where the integral kernel $\overline{K}:\mathbb{R}^+\times\mathbb{R}^+\to\mathbb{R}$ is defined as

$$\overline{K}(r,s) := (rs)^d\int_{S^{d-1}}\int_{S^{d-1}}\langle\xi,\eta\rangle\frac{1}{L}\sum_{l=1}^{L}p_{t_l}(r\xi,s\eta)d\xi d\eta, \tag{84}$$

with $p_{t_l}(u,v)$ denoting the joint density function of the random vector $(\boldsymbol{r}_{12}(t_l),\boldsymbol{r}_{13}(t_l))$ and $\mathbb{S}^{d-1}$ denoting the unit sphere in $\mathbb{R}^d$. The coercivity constant satisfies that

$$c_{\mathcal{H}_K} = \frac{N-1}{N^2} + \frac{(N-1)(N-2)}{N^2}\kappa_{\mathcal{H}_K}.$$

Therefore, if the integral kernel $\overline{K}$ is positive definite, i.e., $\kappa_{\mathcal{H}} \geq 0$, then the coercivity condition holds on $\mathcal{H}_K$ with $c_{\mathcal{H}_K} \geq \frac{N-1}{N^2}$.

In the case of $L = 1$ where the initial distributions of the agents are exchangeable Gaussian, it is proven in (Lu et al., 2021) that $\kappa_{\mathcal{H}_K} > 0$ provided $\mathcal{H}_K$ can be compactly embedded into $L^2([0,R];\tilde{\rho}_T^1;\mathbb{R})$. Back to our setting, the previous results indicate that the coercivity condition (55) is satisfied with the coercivity constant independent of N if

- $\mathcal{H}_K$ is finite dimensional
- $\mathcal{H}_K$ is a subspace of Sobolev space $W_2^s([0,R])$ for $s > \frac{1}{2}$ (see def in (86)).
- the kernel K is a C^∞ Mercer kernel.

The space $\mathcal{H}_K$ in the last two examples can be embedded compactly into $C([0,R])$(Cucker and Smale, 2002) and therefore into the space $L^2([0,R];\tilde{\rho}_T^1;\mathbb{R})$. In these scenarios, the condition number of the inverse problem is uniformly bounded below and is independent of the number of agents in the system.

We also prove that $\overline{K}(r,s)$ is positive definite if the initial distribution of each agent is drawn i.i.d according to a probability measure on $\mathbb{R}^d$. This indicates that the coercivity constant $c_{\mathcal{H}_K} \geq \frac{N-1}{N^2}$ as long as $\mathcal{H}_K$ is a subspace of $L^2([0,R];\tilde{\rho}_T^1;\mathbb{R})$. The generalization for the case $L > 1$ is difficult for deterministic systems, due to the implicit solutions to the systems and the richness of collective behaviors which cause grand challenges to analyzing distributions in a unified way.

However, as the numerical results and relevant discussions in (Lu et al., 2019, 2021), we believe that the coercivity condition is "generally" satisfied for various systems and initial distributions for the case $L > 1$. We also refer the reader to (Lu et al., 2020) for the study of coercivity conditions in stochastic systems.

3.7 Analysis of computational complexity

To compute the posterior mean and variance, the direct construction of the covariance matrix K_ϕ requires $\mathcal{O}(N^4M^2L^2d)$ operations and the direct inversion of the covariance matrix requires $\mathcal{O}((NMLd)^3)$ operations. Theoretically, we prove the scalability in M: for example, when $\gamma = \frac{1}{2}$, for the accuracy ϵ, it is of the order $\mathcal{O}((\frac{1}{\epsilon})^6)$, independent of the ambient dimension dN. In our numerical experiments, we used direct inversion of kernel matrices as we focused on the scarce and noisy data regime. In our numerical sections, we test our approach on systems with dimensions ranging from 10 to 60.

The most expensive computational part of the full GP model is on constructing the covariance matrix K_ϕ and inverting it. This is a well-known limitation of the GP approach. There are many possible ways of overcoming the computational bottleneck. Currently, we are investigating the use of a sparse conjugate gradient method (CG) to solve the linear system which does not require assembling the covariance matrix and uses an iterative method to get the estimator. Our Representer theorem implies that the covariance matrix K_ϕ has a special sparse structure depending on the covariance kernel we use, which allows us to efficiently compute the matrix-vector multiplication used in each iteration of CG, similar to the ideas used in the Kalman filter. The total cost can be reduced to $\mathcal{O}(N^2MLdp)$ where p is the number of total iterations (usually a few hundred steps). We refer the reader to (Gu et al., 2022) for the preliminary investigation in first-order systems.

4 Numerical Examples

Numerical setup. We simulate the trajectory data on the time interval $[0,T]$ with given i.i.d initial conditions generated from the probability measures specified for each system. For the training data sets, we generate M trajectories and observe each trajectory at L equidistant times $0 = t_1 < t_2 < \cdots < t_L = T$. All ODE systems are evolved using ode15s in MATLAB®2020a with a relative tolerance at 10^{-5} and absolute tolerance at 10^{-6}. We apply the *minimize* function in the GPML package[2] to train the parameters using conjugate gradient optimization with the partial derivatives shown in Proposition 4, and set the maximum number of function evaluations to 600.

[2]Carl Edward Rasmussen & Hannes Nickisch (http://gaussianprocess.org/gpml/code)

Table 3: Short Notations

Notation	Definition
GPs	Gaussian Processes
GPR	Gaussian Process Regression
RKHS	Reproducing Kernel Hilbert Space
KRR	Kernel Ridge Regression
IC	Initial Condition

Choice of the covariance function. We choose the Matérn covariance function restricted on $[0, R] \times [0, R]$ for the Gaussian process priors in our numerical experiments, i.e.,

$$K_\theta(r, r') = s_\phi^2 \frac{2^{1-\nu}}{\Gamma(\nu)} (\frac{\sqrt{2\nu}|r - r'|}{\omega_\phi})^\nu B_\nu (\frac{\sqrt{2\nu}|r - r'|}{\omega_\phi}), \tag{85}$$

where the parameter $\nu > 0$ determines the smoothness; $\Gamma(\nu)$ is the Gamma function; B_ν is the modified Bessel function of the second kind; and the hyper-parameters $\theta = \{s_\phi^2, \omega_\phi\}$ quantify the amplitude and scales.

The Reproducing Kernel Hilbert Space (RKHS), $\mathcal{H}_{\text{Matérn}}$, associated with this Matérn kernel is norm-equivalent to the Sobolev space $W_2^{\nu+1/2}([0, R])$ defined by

$$W_2^{\nu+1/2}([0, R]) := \Big\{ f \in L^2([0, R]) : \|f\|^2_{W_2^{\nu+1/2}} := \sum_{\beta \in \mathbb{N}_0^1 : |\beta| \le \nu+1/2} \|D^\beta f\|^2_{L_2} < \infty \Big\}. \tag{86}$$

That is to say, $\mathcal{H}_{\text{Matérn}} = W_2^s([0, R])$ as a set of functions, and there exist constants $c_1, c_2 > 0$ such that

$$c_1 \|f\|_{W_2^{\nu+\frac{1}{2}}} \le \|f\|_{\mathcal{H}_{\text{Matérn}}} \le c_2 ||f||_{W_2^{\nu+\frac{1}{2}}}, \quad \forall f \in \mathcal{H}_{\text{Matérn}}. \tag{87}$$

In other words, $\mathcal{H}_{\text{Matérn}}$ consists of functions that are differentiable up to order ν and weak differentiable up to order $s = \nu + \frac{1}{2}$.

Baseline comparisons We perform comparisons with approaches that learn the right-hand side function of (10) directly from trajectory data: the first one is SINDy (Brunton et al., 2016), which aims at finding a sparse representation for each row of governing equations in a (typically large) dictionary; the second one is regression using Feed-Forward Neural networks (FNN), for which we use the MATLAB® 2021a Deep Learning Toolbox™. To evaluate the performance, we compare the trajectory prediction errors of the estimators. We also perform a comparison with the previous least square approach for learning ϕ, see Table 11.

Overview of the numerical results

- The proposed algorithm performs *simultaneous* accurate estimations of $\boldsymbol{\alpha}$ in the non-collective force functions and ϕ from a *small* amount of *noisy* trajectory data, even in the cases where $\boldsymbol{F}$ depends *nonlinearly* on $\boldsymbol{\alpha}$ (See Example 4.1). Although we are dealing with non-convex optimization in our training step, our algorithm works well in tuning the hyper-parameters when the initialization is within an appropriate range. We find that learning ϕ is more challenging, since finding α is a parameter estimation problem with a small number of unknowns (2 to 5 unknowns) while finding ϕ is a nonparametric inference

problem and suffers from the possible ill-posedness of the inverse problem. We show in Example 4.1 (Table 5) the existence of outliers in learning ϕ from noise-free data, while we do not observe this phenomenon for $\boldsymbol{\alpha}$ and the cases using noisy training data. It suggests that regularization is needed in the noise-free case.

- Our numerical results show that the estimation errors for both $\boldsymbol{\alpha}$ and ϕ decrease as the size of training data increases. It remains elusive regarding the role of N, M, and L in determining the size of "effective" samples, which serves as the core challenge in learning complex systems. In addition, we would like to point out that the hyper-parameters for the Matérn kernel are known to be unidentifiable (Zhang, 2004; Tang et al., 2021). Our learning theory treats M as the effective sample size and N, L fixed. We address how to choose the prior as $M \to \infty$ so as to achieve the optimal convergence of estimators. We leave all other regimes for future work.

- The marginal posterior variances obtained in our learning approach quantify the reliability of estimated kernels and are fairly small in the region well-explored by the training data. We also observe that the estimators can extrapolate well in the regions which are not explored by the training data. We impute this extrapolation property to the powerful training procedure of GPR, which learns a covariance kernel function that achieves an automatic trade-off between data-fit and model complexity. For the fixed sample size, the width of the uncertainty band increases as the noise level increases. We remark that this can also serve as a sign of the model mismatch error if the system is applied to fit a real dataset.

- Predicting long term behavior of complex systems is known to be very challenging. Our estimators are shown to have good performance in prediction and generalization. The occasional large prediction errors that happened in a larger time interval may be caused by the propagation of estimation errors. We still think the performance is satisfactory since we only have very limited and noisy training data. Even in cases where the prediction errors are relatively large, the estimators can predict remarkably accurate collective behaviors of the agents, e.g. the consensus in the opinion dynamics, the flocking behavior in the Cuker-Smale dynamics, and the milling pattern in the fish milling dynamics.

- Besides the SINDy and FNN models, we also conduct a comparison with the learning approach proposed in previous work (Lu et al., 2019; Zhong et al., 2020) when ϕ is the only unknown term in the governing equation (see Example 4.2.)

4.1 Example 1: Opinion dynamics (OD) with stubborn agents

We consider the Taylor model (Taylor, 1968), which models the collective dynamics of continuous opinion exchange in the presence of stubborn agents. It is a first-order system of N interacting agents, and each agent i is characterized by a continuous opinion variable $x_i \in \mathbb{R}$. The dynamics of opinion exchange are governed by the following first-order equation,

$$\dot{\boldsymbol{x}}_i \;=\; \boldsymbol{F}_i(\boldsymbol{x}_i, \boldsymbol{\alpha}) + \sum_{i'=1}^{N} \frac{1}{N} \phi(\|\boldsymbol{x}_{i'} - \boldsymbol{x}_i\|)(\boldsymbol{x}_{i'} - \boldsymbol{x}_i), \tag{88}$$

where

$$\phi(r) = \begin{cases} 2.5r & \text{if } 0 \le r < 0.4 \\ 1 & \text{if } 0.4 \le r < 0.6 \\ 2.5 - 2.5r & \text{if } 0.6 \le r < 1 \\ 0 & \text{if } r \ge 1 \end{cases} \tag{89}$$

and

$$\boldsymbol{F}_i(\boldsymbol{x}_i, \boldsymbol{\alpha}) = \begin{cases} -\kappa(\boldsymbol{x}_i - P_i) & \text{if agent } i \text{ is stubborn with bias } P_i \\ 0 & \text{otherwise} \end{cases} \tag{90}$$

The interaction kernel ϕ encodes the non-repulsive interactions between agents: all agents aim to align their opinions to their connected neighbors according to distanced-based attractive influences. The non-collective force $\boldsymbol{F}(\boldsymbol{x}_i, \boldsymbol{\alpha})$ describes the additional influence induced by the stubbornness: the stubborn agents have strong desires to follow their biases P_i, and κ controls the rate of convergence towards their biases. The stubborn agents may cause a major effect on the collective opinion formation process. If $\kappa = 0$, then stubborn agents do not follow their biases and behave as regular agents.

We are interested in learning the parameters $\boldsymbol{\alpha} = (P_1, P_2, P_3, \kappa)$ and interaction kernel ϕ from trajectory data. Note that this first-order system is a special case of the second-order system (12) with $m_i = 0$ for all i, and $\boldsymbol{F}_i(\boldsymbol{x}_i, \dot{\boldsymbol{x}}_i, \boldsymbol{\alpha}) = -\dot{\boldsymbol{x}}_i + \boldsymbol{F}_i(\boldsymbol{x}_i, \boldsymbol{\alpha})$. In this example, the unknown scalar parameters in $\boldsymbol{\alpha}$ are nonlinear with respect to the non-collective force function and the interaction kernel $\phi \notin \mathcal{H}_{\text{Matérn}}$.

The training data $(\mathbb{X}_M, \mathbb{V}_{\sigma^2,M})$ is generated with parameters shown in Table 4, and the observations are made in the time interval $[0, 15]$ with different size of observations $\{M, L\}$, and different noise level σ.

Table 4: System parameters in the opinion dynamics

d	N	$[0; T; T_f]$	$\alpha = (P_1, P_2, P_3, \kappa)$	μ_0
1	10	$[0, 15, 20]$	$(1, 0, -1, 10)$	$\text{Unif}([-1, 1])$

We initialize the parameters $(\sigma, P_1, P_2, P_3, \kappa) = (1/2, 1/2, 1/2, 1/2, 1/2)$. Table 5 shows the errors of the estimations for $\boldsymbol{\alpha}$ and $\phi(r)$ in 10 independent trials of experiments. The results demonstrate that our algorithm can produce an accurate estimation of the parameters $(\sigma, P_1, P_2, P_3, \kappa)$ from both noise-free and noisy training data. For the estimation of $\phi(r)$, even though ϕ is not in the RKHS generated by the Matérn kernel, our algorithm still provides us with faithful prediction in the region the training data covers, see Figure 1 (a). At the region around $r = 0$, we see the approximation is not as good as in other regions. We impute this phenomenon to the fact that $\phi(r)$ is weighted by $\boldsymbol{r}$ in the model (88), thus we lose the information of ϕ when $\boldsymbol{r}$ is close to zero. However, we expect that our estimators will produce accurate trajectories since they are generated by $\phi(r)\boldsymbol{r}$, and Figure 1 (b) supports this intuition.

The comparison between the trajectories generated by the parameters $\boldsymbol{\alpha}$ and interaction kernel ϕ, and the estimated parameters $\hat{\boldsymbol{\alpha}}$ and interaction kernel $\hat{\phi}$, is shown in Table 6. We can see that in both the training time interval $[0, 15]$ and future time interval $[15, 20]$, the estimators can produce accurate approximations of the trajectories and the performance becomes better when we increase the size of training data (M or L).

4.2 Example 2: Fish-Milling (FM) dynamics with friction force

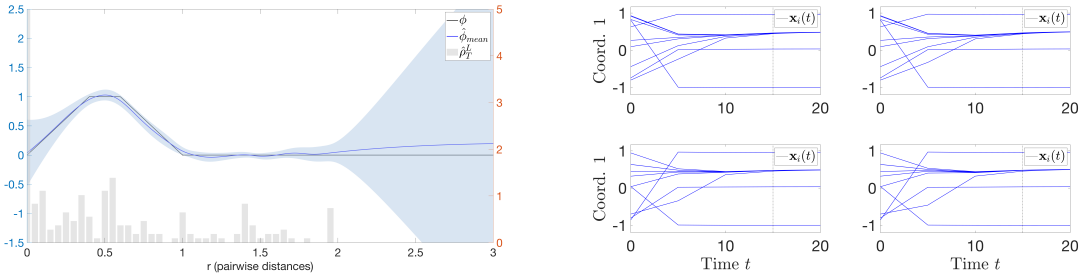
We consider the D'orsogma model (D'Orsogna et al., 2006; Chuang et al., 2007) which describes the motion of N self-propelled particles powered by biological or mechanical motors under

[1]omit 2 trails in the 10 independent learning trails for errors in ϕ and corresponding trajectories, the result with all 10 trials are shown in the brackets below

[2]omit 1 trail in the 10 independent learning trails for errors in ϕ and corresponding trajectories, the result with all 10 trials are shown in the brackets below

Table 5: Means and standard deviations of the errors of $\hat{\boldsymbol{\alpha}}$ (including $\hat{\sigma}$ when noise exists) and $\hat{\phi}$ for different settings

$\{N, M, L, \sigma\}$	$\|\hat{\boldsymbol{\alpha}} - \boldsymbol{\alpha}\|_\infty$	$\|\hat{\phi} - \phi\|_\infty$
$\{10, 3, 4, 0\}$ [1]	$5.1 \cdot 10^{-3} \pm 8.2 \cdot 10^{-3}$	$1.0 \cdot 10^{-1} \pm 2.2 \cdot 10^{-2}$ $(6.0 \cdot 10^{-1} \pm 2.2 \cdot 10^{-2})$
$\{10, 3, 8, 0\}$	$4.2 \cdot 10^{-4} \pm 5.4 \cdot 10^{-3}$	$7.5 \cdot 10^{-2} \pm 2.5 \cdot 10^{-2}$
$\{10, 6, 4, 0\}$ [2]	$2.8 \cdot 10^{-3} \pm 9.8 \cdot 10^{-3}$	$7.6 \cdot 10^{-2} \pm 2.2 \cdot 10^{-2}$ $(1.7 \cdot 10^{-1} \pm 3.0 \cdot 10^{-1})$
$\{10, 6, 4, 0.01\}$	$1.6 \cdot 10^{-3} \pm 4.7 \cdot 10^{-3}$	$5.9 \cdot 10^{-2} \pm 2.8 \cdot 10^{-2}$
$\{10, 6, 4, 0.03\}$	$4.1 \cdot 10^{-3} \pm 1.1 \cdot 10^{-2}$	$1.4 \cdot 10^{-1} \pm 8.3 \cdot 10^{-2}$
$\{10, 6, 4, 0.05\}$	$7.2 \cdot 10^{-3} \pm 2.2 \cdot 10^{-2}$	$1.9 \cdot 10^{-1} \pm 1.3 \cdot 10^{-1}$



(a) OD: vs learned kernel

(b) versus predicted model

Figure 1: Learning OD ($\{N, M, L, \sigma\} = \{10, 6, 4, 0.05\}$) using the Matérn kernel. (a): predictive mean $\hat{\phi}$ of the kernel, and two-standard-deviation band (light blue color) around the mean. The grey bars represent the empirical density of the ρ_T^L. (b): the true (left) versus predicted (right) trajectories using $\hat{\boldsymbol{\alpha}}$ and $\hat{\phi}$ with initial conditions of training data (top) and testing data (bottom).

Table 6: The trajectory prediction errors for different settings.

$\{N, M, L, \sigma\}$	Training IC $[0, 15]$	Training IC $[15, 20]$	New IC $[0, 15]$	New IC $[15, 20]$
$\{10, 3, 4, 0\}$	$1.2 \cdot 10^{-2} \pm 9.3 \cdot 10^{-3}$	$2.3 \cdot 10^{-2} \pm 4.2 \cdot 10^{-2}$	$1.4 \cdot 10^{-2} \pm 7.1 \cdot 10^{-3}$	$2.1 \cdot 10^{-2} \pm 3.2 \cdot 10^{-2}$
$\{10, 3, 8, 0\}$	$8.1 \cdot 10^{-3} \pm 3.4 \cdot 10^{-3}$	$7.0 \cdot 10^{-3} \pm 5.4 \cdot 10^{-3}$	$8.3 \cdot 10^{-3} \pm 5.3 \cdot 10^{-3}$	$5.9 \cdot 10^{-3} \pm 4.4 \cdot 10^{-3}$
$\{10, 6, 4, 0\}$	$1.1 \cdot 10^{-2} \pm 6.2 \cdot 10^{-3}$	$8.0 \cdot 10^{-3} \pm 7.0 \cdot 10^{-3}$	$1.8 \cdot 10^{-2} \pm 1.8 \cdot 10^{-2}$	$6.9 \cdot 10^{-3} \pm 4.4 \cdot 10^{-3}$
$\{10, 6, 4, 0.01\}$	$3.4 \cdot 10^{-2} \pm 2.0 \cdot 10^{-2}$	$2.7 \cdot 10^{-2} \pm 2.0 \cdot 10^{-2}$	$4.2 \cdot 10^{-2} \pm 2.0 \cdot 10^{-2}$	$4.1 \cdot 10^{-2} \pm 4.4 \cdot 10^{-2}$
$\{10, 6, 4, 0.03\}$	$6.6 \cdot 10^{-2} \pm 3.3 \cdot 10^{-2}$	$5.7 \cdot 10^{-2} \pm 4.2 \cdot 10^{-2}$	$7.1 \cdot 10^{-2} \pm 3.1 \cdot 10^{-2}$	$3.9 \cdot 10^{-2} \pm 1.7 \cdot 10^{-2}$
$\{10, 6, 4, 0.05\}$	$1.1 \cdot 10^{-1} \pm 4.2 \cdot 10^{-2}$	$8.0 \cdot 10^{-2} \pm 6.4 \cdot 10^{-2}$	$1.2 \cdot 10^{-1} \pm 5.9 \cdot 10^{-2}$	$6.9 \cdot 10^{-2} \pm 4.1 \cdot 10^{-2}$

frictional forces: for $i = 1, \cdots, N$,

$$m_i \ddot{\boldsymbol{x}}_i = \boldsymbol{F}_i(\boldsymbol{x}_i, \dot{\boldsymbol{x}}_i, \boldsymbol{\alpha}) + \sum_{i'=1}^{N} \frac{1}{N} \phi(\|\boldsymbol{x}_{i'} - \boldsymbol{x}_i\|)(\boldsymbol{x}_{i'} - \boldsymbol{x}_i), \tag{91}$$

$$\boldsymbol{F}_i(\boldsymbol{x}_i, \dot{\boldsymbol{x}}_i, \boldsymbol{\alpha}) = (\gamma - \beta|\dot{\boldsymbol{x}}_i|^2)\dot{\boldsymbol{x}}_i. \tag{92}$$

The form of (91) is derived using Newton's law with the right hand side of (91) describing the three forces acting on each agent: self-propulsion with strength γ, nonlinear drag with strength β, and social interactions determined by ϕ. This system can produce a rich variety of collective patterns: in our numerical example, we consider the interaction kernel that is derived from the Morse-type potential

$$\phi(r) = \frac{1}{r}\bigg[- \frac{C_{rp}}{l_{rp}} e^{-\frac{r}{l_{rp}}} + \frac{C_a}{l_a} e^{-\frac{r}{l_a}} \bigg], \tag{93}$$

where l_a, l_{rp} represent the attractive and repulsive potential ranges and C_a, C_{rp} represent the respective amplitudes. Since this kernel is singular at $r = 0$, we truncate it at $r_0 = 0.05$ with a function of the form ae^{-br} to ensure that the new function has a continuous derivative. We assume that we do not have knowledge of the parametric form of ϕ, γ, and β, and our goal is to learn them from the trajectory data.

As mentioned above, the training data $(\mathbb{Y}_M, \mathbb{Z}_{\sigma^2,M})$ is generated with different numbers of agents N and the parameters shown in Table 7, and the observations are made in the time interval $[0, 5]$ with different sizes $\{M, L\}$ and different amounts of additive noise σ.

Table 7: System parameters in the fish milling dynamics

d	m_i	$[0; T; T_f]$	$\boldsymbol{\alpha} = (\gamma, \beta)$	(C_{rp}, l_{rp})	(C_a, l_a)	$\mu_0^{\boldsymbol{x}}$	$\mu_0^{\boldsymbol{v}}$
2	1	$[0; 5; 10]$	$(1.5, 0.5)$	(0.5,0.5)	(4,4)	$\mathcal{U}([-0.5, 0.5]^2)$	$(0, 0)$

We initialize the parameters $(\gamma, \beta) = (1, 1)$, and $\sigma = 1$ for the cases with noisy data. The errors of the estimations for $\boldsymbol{\alpha}$ after our training procedure and the learned ϕ are shown in Table 8. In this model, ϕ is in the RKHS generated by the chosen Matérn kernel. We can see that our estimators produced faithful approximations to the kernel based on the results, see Figure 2 (a). We also compare the discrepancy between the trajectories (evolved using α, ϕ) and predicted trajectories (evolved using $\hat{\alpha}$, $\hat{\phi}$) on both the training time interval $[0, T]$ and on the future time interval $[T, T_f]$, over two different sets of initial conditions (IC) – one taken from the training data, and one consisting of new samples from the same initial distribution, see the results of different cases in Table 9 and Figure 2 (b)-(c).

Even if the trajectory prediction errors can go up to $O(10^{-1})$ with the presence of a relatively large noise for the systems with $N = 10$, our estimators provided faithful predictions to most of the agents in the system, and the milling pattern as shown in Figure 2(c).

Baseline Comparisons For the case where $\{N, M, L, \sigma\} = \{5, 1, 9, 0\}$, we compare our results with the SINDy model and the FNN models: for the SINDy model, we apply a reasonably large dictionary of monomials up to order 2 and sines and cosines of frequencies $\{k\}_{k=1}^{10}$, and fit the system $\dot{\boldsymbol{Y}} = [\boldsymbol{V}, \boldsymbol{Z}]^T = \tilde{\mathbf{f}}_\phi(\boldsymbol{Y})$ with the same training data $\{\mathbb{Y}_M, \mathbb{Z}_{\sigma^2,M}\}$; for the FNN model, we consider a three-layer FNN with $[40, 40, 20]$ hidden units. The results are shown in Figure 3 (a),(b) and Table 10. Since we only train the models with a small amount of data (9 observations, 0:0.625:5 in the training time interval [0,5]), both SINDy and FNN fail to provide accurate trajectory predictions on the training time interval and perform even worse in the testing time interval [5,10], since they do not include the physical information of the fish milling system in contrast to our method.

Table 8: Means and standard deviations of the errors of $\hat{\boldsymbol{\alpha}}$ (including $\hat{\sigma}$ when noise exists) and $\hat{\phi}$ for different settings

$\{N, M, L, \sigma\}$	$\|\hat{\boldsymbol{\alpha}} - \boldsymbol{\alpha}\|_\infty$	$\|\hat{\phi} - \phi\|_\infty$
$\{10, 1, 3, 0\}$	$3.1 \cdot 10^{-4} \pm 1.5 \cdot 10^{-4}$	$2.6 \cdot 10^{-2} \pm 4.3 \cdot 10^{-3}$
$\{10, 1, 9, 0\}$	$1.2 \cdot 10^{-4} \pm 1.8 \cdot 10^{-4}$	$2.3 \cdot 10^{-2} \pm 3.1 \cdot 10^{-3}$
$\{10, 3, 3, 0\}$	$2.3 \cdot 10^{-4} \pm 1.7 \cdot 10^{-4}$	$2.5 \cdot 10^{-2} \pm 3.4 \cdot 10^{-3}$
$\{5, 3, 3, 0\}$	$3.0 \cdot 10^{-4} \pm 1.6 \cdot 10^{-4}$	$2.4 \cdot 10^{-2} \pm 3.3 \cdot 10^{-3}$
$\{10, 3, 3, 0.01\}$	$8.5 \cdot 10^{-4} \pm 2.6 \cdot 10^{-3}$	$2.5 \cdot 10^{-2} \pm 5.0 \cdot 10^{-3}$
$\{10, 3, 3, 0.05\}$	$3.0 \cdot 10^{-3} \pm 1.3 \cdot 10^{-2}$	$1.7 \cdot 10^{-2} \pm 8.7 \cdot 10^{-3}$
$\{10, 3, 3, 0.1\}$	$5.7 \cdot 10^{-3} \pm 2.7 \cdot 10^{-2}$	$3.0 \cdot 10^{-2} \pm 1.7 \cdot 10^{-2}$

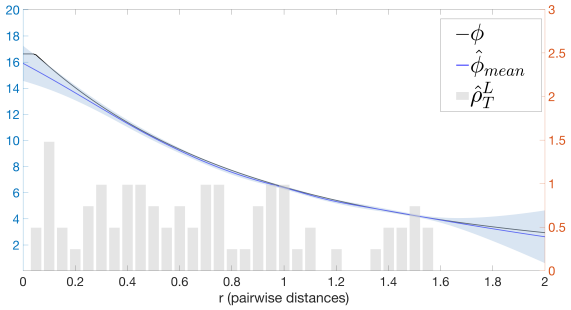
Table 9: The trajectory prediction errors for different settings of FM dynamics.

$\{N, M, L, \sigma\}$	Training IC $[0, 5]$	Training IC $[5, 10]$	New IC $[0, 5]$	New IC $[5, 10]$
$\{10, 1, 3, 0\}$	$2.6 \cdot 10^{-2} \pm 9.7 \cdot 10^{-3}$	$6.9 \cdot 10^{-2} \pm 3.3 \cdot 10^{-2}$	$2.7 \cdot 10^{-2} \pm 7.7 \cdot 10^{-3}$	$1.1 \cdot 10^{-1} \pm 1.0 \cdot 10^{-1}$
$\{10, 1, 9, 0\}$	$1.6 \cdot 10^{-2} \pm 8.1 \cdot 10^{-3}$	$4.2 \cdot 10^{-2} \pm 2.1 \cdot 10^{-2}$	$1.4 \cdot 10^{-2} \pm 3.7 \cdot 10^{-3}$	$3.7 \cdot 10^{-2} \pm 2.2 \cdot 10^{-2}$
$\{10, 3, 3, 0\}$	$1.4 \cdot 10^{-2} \pm 9.1 \cdot 10^{-3}$	$4.4 \cdot 10^{-2} \pm 3.5 \cdot 10^{-2}$	$1.3 \cdot 10^{-2} \pm 9.4 \cdot 10^{-3}$	$4.8 \cdot 10^{-2} \pm 3.2 \cdot 10^{-2}$
$\{5, 5, 6, 0\}$	$1.8 \cdot 10^{-3} \pm 6.1 \cdot 10^{-3}$	$4.3 \cdot 10^{-2} \pm 3.0 \cdot 10^{-1}$	$1.5 \cdot 10^{-3} \pm 2.8 \cdot 10^{-3}$	$2.3 \cdot 10^{-2} \pm 5.8 \cdot 10^{-1}$
$\{5, 3, 3, 0\}$	$2.7 \cdot 10^{-3} \pm 2.4 \cdot 10^{-3}$	$2.3 \cdot 10^{-2} \pm 2.5 \cdot 10^{-2}$	$2.5 \cdot 10^{-3} \pm 1.5 \cdot 10^{-3}$	$9.7 \cdot 10^{-2} \pm 1.5 \cdot 10^{-1}$
$\{10, 3, 3, 0.01\}$	$2.6 \cdot 10^{-2} \pm 8.5 \cdot 10^{-3}$	$7.2 \cdot 10^{-2} \pm 3.7 \cdot 10^{-2}$	$2.7 \cdot 10^{-2} \pm 1.1 \cdot 10^{-2}$	$7.9 \cdot 10^{-2} \pm 3.8 \cdot 10^{-2}$
$\{10, 3, 3, 0.05\}$	$1.3 \cdot 10^{-1} \pm 4.3 \cdot 10^{-2}$	$3.4 \cdot 10^{-1} \pm 1.8 \cdot 10^{-1}$	$1.2 \cdot 10^{-1} \pm 4.6 \cdot 10^{-2}$	$3.2 \cdot 10^{-1} \pm 1.1 \cdot 10^{-1}$
$\{10, 3, 3, 0.1\}$	$2.6 \cdot 10^{-1} \pm 1.0 \cdot 10^{-1}$	$7.0 \cdot 10^{-1} \pm 3.7 \cdot 10^{-1}$	$2.2 \cdot 10^{-1} \pm 1.1 \cdot 10^{-1}$	$5.8 \cdot 10^{-1} \pm 2.4 \cdot 10^{-1}$

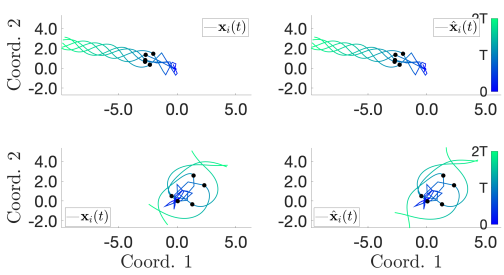
Table 10: Baseline comparison. The relative trajectory prediction errors.

Approach	Training time interval	Testing time interval
GPs	$\mathbf{3.6 \cdot 10^{-3} \pm 2.5 \cdot 10^{-3}}$	$\mathbf{2.4 \cdot 10^{-1} \pm 3.1 \cdot 10^{-1}}$
SINDy	$9.4 \cdot 10^{-1} \pm 3.8 \cdot 10^{-1}$	$1.2 \cdot 10^{0} \pm 4.7 \cdot 10^{-1}$
FNN	$2.2 \cdot 10^{0} \pm 1.3 \cdot 10^{0}$	$3.1 \cdot 10^{0} \pm 1.7 \cdot 10^{0}$

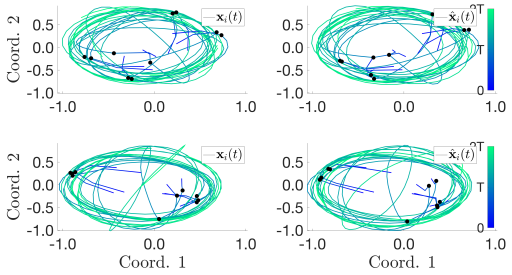
Comparison with the previous methods Here, we also provide another comparison with one recently proposed method on the data-driven discovery of interacting particle system (Lu et al., 2019; Zhong et al., 2020), where they also incorporate the information of the physical structures of the model but only assume ϕ is unknown in the system, and $\boldsymbol{\alpha}$ is given. Therefore, to compare with this previous method, we fixed the parameters $(\boldsymbol{\alpha}, \theta)$ in our model with the true parameters $\boldsymbol{\alpha}$ and a guessed parameter for θ, and we predict ϕ with the fixed parameters $(\boldsymbol{\alpha}, \theta)$ without training procedure.



(a) FM: vs learned kernel



(b) $\{N, M, L, \sigma\} = \{5, 5, 6, 0\}$



(c) $\{N, M, L, \sigma\} = \{10, 3, 3, 0.1\}$

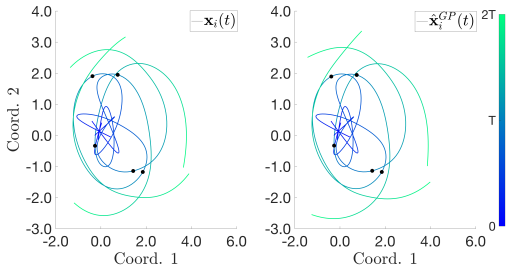
Figure 2: Learning Fish Milling (FM) using the Matérn kernel. (a): ϕ versus the posterior mean $\hat{\phi}_{mean}$, with a two-standard-deviation band (light blue color) around the mean. The grey bars represent the histogram of pairwise distances, with density value shown in the orange axis. (b),(c): The true (left) versus predicted (right) trajectories using $\hat{\boldsymbol{\alpha}}$ and $\hat{\phi}$ with initial conditions of training data (top) and testing data (bottom).

We consider the case where $\{N, M, L\} = \{5, 5, 6\}$ and $\sigma = 0$ or 0.01. Using the previous method, we apply piecewise linear polynomials with $n = 18$ basis functions to approximate ϕ on the support $[0, R] = [0, 4.66]$ by solving a least square problem, while we consider the function space $\mathcal{H}_{\text{Matérn}}$ with $\theta = (10^2, 0.1)$ using our new method. By Theorem 14, the posterior mean estimator obtained is approximately the least-square solution when the noise is very small. Noise in fact serves a role of regularization in our method. We compare the errors of $\hat{\phi}$ using the supremum norm (post-smoothing techniques are applied to piecewise linear estimators) and present the relative trajectory prediction errors for both estimators.

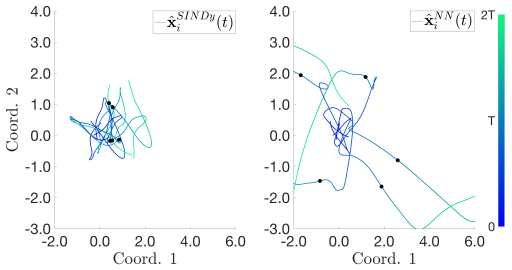
Table 11: The trajectory prediction errors for different models of FM dynamics $\{N, M, L\} = \{5, 5, 6\}$.

Method	σ	$\|\hat{\phi} - \phi\|_\infty$	Training IC $[0, 5]$	Training IC $[5, 10]$	New IC $[0, 5]$	New IC $[5, 10]$
previous	0	$1.9 \cdot 10^{-1} \pm 2.9 \cdot 10^{-2}$	$1.3 \cdot 10^{-1} \pm 2.8 \cdot 10^{-2}$	$2.7 \cdot 10^{-1} \pm 1.1 \cdot 10^{-1}$	$1.4 \cdot 10^{-1} \pm 3.8 \cdot 10^{-2}$	$3.5 \cdot 10^{-1} \pm 1.5 \cdot 10^{-1}$
now	0	$\mathbf{3.4 \cdot 10^{-2} \pm 5.5 \cdot 10^{-3}}$	$\mathbf{2.4 \cdot 10^{-3} \pm 2.5 \cdot 10^{-3}}$	$\mathbf{1.5 \cdot 10^{-1} \pm 5.6 \cdot 10^{-1}}$	$\mathbf{2.0 \cdot 10^{-3} \pm 1.4 \cdot 10^{-3}}$	$\mathbf{1.9 \cdot 10^{-1} \pm 4.9 \cdot 10^{-1}}$
previous	0.01	$1.9 \cdot 10^{-1} \pm 3.5 \cdot 10^{-2}$	$1.5 \cdot 10^{-1} \pm 3.6 \cdot 10^{-2}$	$2.8 \cdot 10^{-1} \pm 9.4 \cdot 10^{-2}$	$1.3 \cdot 10^{-1} \pm 3.4 \cdot 10^{-2}$	$3.1 \cdot 10^{-1} \pm 1.5 \cdot 10^{-1}$
now	0.01	$\mathbf{2.8 \cdot 10^{-2} \pm 1.6 \cdot 10^{-2}}$	$\mathbf{6.9 \cdot 10^{-3} \pm 2.5 \cdot 10^{-2}}$	$\mathbf{1.1 \cdot 10^{-1} \pm 8.3 \cdot 10^{-1}}$	$\mathbf{3.6 \cdot 10^{-3} \pm 2.6 \cdot 10^{-3}}$	$\mathbf{1.5 \cdot 10^{-1} \pm 7.2 \cdot 10^{-1}}$

From the results shown in Table 11, we can see that our new approach has better performance than the previous approach, given the limited size of training data. One drawback of the previous approach lies in selecting the optimal number of bases to minimize the error. We have tried



(a) True versus Our Model in FM dynamics

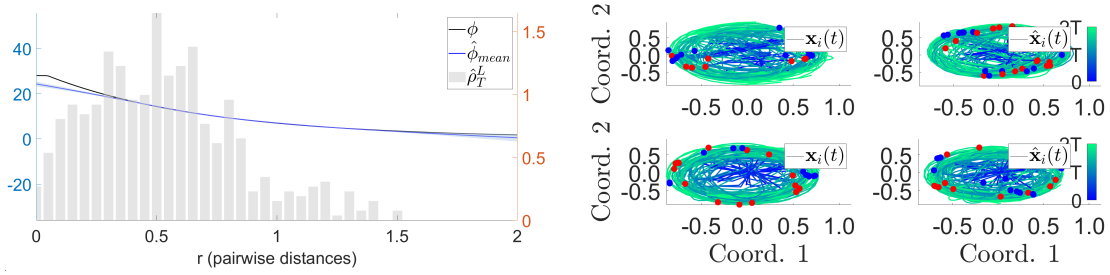


(b) Comparison with SINDy and FNN in FM dynamics

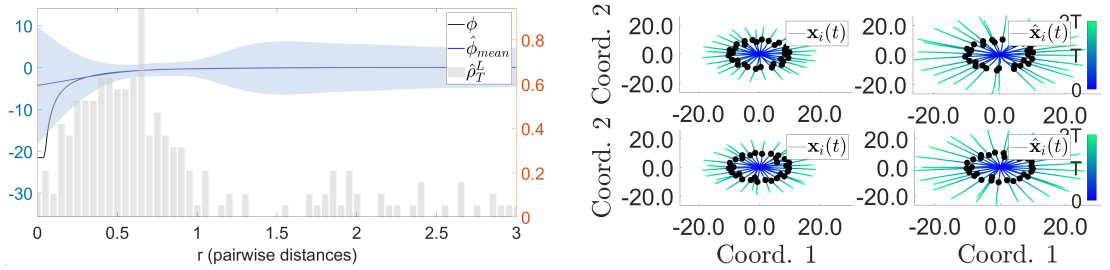
Figure 3: Top: Learning FM dynamics from training data $\{N, M, L, \sigma\} = \{5, 1, 9, 0.1\}$. (a): the true trajectory versus the prediction from our GP model. (b): the SINDy model and the FNN model trajectories.

different n (up to 100) for the previous approach, but none of them can provide a significantly better result than what we have shown here. In contrast, the training step of our approach automatically chooses a basis by updating the prior. For noisy data, our approach is equivalent to regularized least squares. The numerical results also show that regularization improves prediction accuracy.

Other collective patterns. The FM system can also display other collective patterns such as double ring and symmetric escape dynamics. Below, we also display the learning results to show our approach can faithfully learn and predict the ground truth from a small set of noisy data in different scenarios and for systems with larger dimensions.



(a) $\{N, M, L, \sigma\} = \{30, 2, 6, 0.1\}$. Double Ring Pattern.



(b) $\{N, M, L, \sigma\} = \{30, 2, 6, 0.1\}$. Symmetric Escape Pattern.

Figure 4: Learning Fish Milling (FM) using the Matérn kernel for systems with $N = 30$. The true versus predicted kernel (left), and the true versus predicted trajectories (right). Each shows unique collective behavior.

Our method faithfully captures the behavior of the system and is capable of robust prediction. While we expect the error in our approximation of the true interaction force, our predictions reflect well the general dynamics and preserve the critical topological properties of each pattern. The learning errors are summarized in Table 12.

In the double ring pattern, we color counterclockwise orbiting agents as red and clockwise orbiting agents as blue. We can see the mixture of directions of orbit characteristic of the double ring pattern. While prediction errors occur in the exact position of the agents, our method has great success in faithfully predicting the orbit type. With very small amounts of data ($M = 2$), our method predicts only one orbit direction incorrectly among all predictions.

In the symmetric escape pattern, we have a repulsive force under which the agents escape outward with straight trajectories. Our method captures this behavior with very little error, despite the vanishing of learning information as r becomes close to 0.

Table 12: Means and standard deviations of the error of $\hat{\boldsymbol{\alpha}}$ and $\hat{\phi}$ for above patterns

Pattern	$\{C_{rp}, l_{rp}, C_a, l_a\}$	$\|\hat{\boldsymbol{\alpha}} - \boldsymbol{\alpha}\|_\infty$	$\|\hat{\phi} - \phi\|_\infty$
Double Ring	$\{0.5, 0.5, 1, 1\}$	$3.17 \cdot 10^{-1} \pm 4.7 \cdot 10^{-1}$	$2.30 \cdot 10^{-1} \pm 8.8 \cdot 10^{-2}$
Symmetric Escape	$\{2, 0.9, 1, 1\}$	$8.50 \cdot 10^{-1} \pm 8.1 \cdot 10^{-2}$	$7.15 \cdot 10^{-1} \pm 3.3 \cdot 10^{-2}$

The above shows the kernel learning errors. For this section, we only use 20 iterations of the maximum likelihood method, converging very quickly to a close approximation. This exhibits the power of even very few iterations of this methodology.

5 Conclusion

We have considered the inverse problem in a particular yet widely used set of interacting agent systems. We provide a GP based approach that converges optimally and avoids the curse of dimensionality, by exploiting the multiple symmetries in these systems. Extensions of our learning approach to more general systems, such as heterogeneous systems with multiple types of agents and external potentials and stochastic systems may be considered. Another direction is to consider the collective inference problem when only distributions of trajectory data are provided.

A Detailed proofs for lemmas and theorems

Proof of Lemma 21. Note that $\left\|K_r\right\|_{\mathcal{H}_K} \leq \kappa$ for any $r \in [0, R]$, we have that

$$\begin{aligned}\|B_M\varphi\|_{\mathcal{H}_K} &\leq \frac{1}{LM}\sum_{l,m=1}^{L,M}\sum_{i=1,i',i''\neq i}^{N}\frac{1}{N^3}\left\|K_{r_{ii'}^{(m,l)}}\right\|_{\mathcal{H}_K}\|\varphi\|_\infty R^2 \\ &\leq \kappa\|\varphi\|_\infty R^2, a.s.\end{aligned}$$

For the second inequality, we have that

$$\begin{aligned}\mathbb{E}\|B_M\varphi\|_{\mathcal{H}_K}^2 &= \mathbb{E}\langle A_M^* A_M\varphi, A_M^* A_M\varphi\rangle_{\mathcal{H}_K} = \langle A^*A\varphi, B\varphi\rangle_{\mathcal{H}_K} = \langle A\varphi, AB\varphi\rangle_{L^2(\boldsymbol{\rho}_X)} \\ &\leq \|A\varphi\|_{L^2(\boldsymbol{\rho}_X)}\|AB\varphi\|_{L^2(\boldsymbol{\rho}_X)} \leq \|\varphi\|_{L^2(\tilde{\rho}_T^L)}\|B\varphi\|_{L^2(\tilde{\rho}_T^L)} \\ &\leq \|B\|_{L^2(\tilde{\rho}_T^L)}\|\varphi\|_{L^2(\tilde{\rho}_T^L)}^2 \leq \kappa^2 R^2\|\varphi\|_{L^2(\tilde{\rho}_T^L)}^2,\end{aligned}$$

where we use Lemma 28 and Equation (51). □

Proof of Lemma 22 . Define the $\mathcal{H}_K$-valued random variable

$$\xi^{(m)} = \frac{1}{L}\sum_{l=1}^{L}\sum_{i=1,i',i''\neq i}^{N}\frac{1}{N^3}K_{r_{ii'}^{(m,l)}}\langle\varphi, K_{r_{ii''}^{(m,l)}}\rangle_{\mathcal{H}_K}\langle \boldsymbol{r}_{ii'}^{(m,l)}, \boldsymbol{r}_{ii''}^{(m,l)}\rangle.$$

Then the random variables $\{\xi^{(m)}\}_{m=1}^{M}$ are i.i.d. According to Lemma 21, we have that

$$\begin{aligned}\|\xi^{(m)}\|_{\mathcal{H}_K} &\leq \kappa R^2\|\varphi\|_\infty,\\ \mathbb{E}\|\xi^{(m)}\|_{\mathcal{H}_K}^2 &\leq \kappa^2 R^2\|\varphi\|_{L^2(\tilde{\rho}_T^L)}.\end{aligned}$$

Note that $B_M\varphi - B\varphi = \frac{1}{M}\sum_{m=1}^{M}(\xi^{(m)} - \mathbb{E}(\xi^{(m)}))$. The conclusion follows by applying Lemma 29 to $\{\xi^{(m)}\}_{m=1}^{M}$. □

Proof of Lemma 23. We introduce an intermediate quantity $(B_M+\lambda)^{-1}B\varphi$ and decompose

$$\begin{aligned}&(B_M+\lambda)^{-1}B_M\varphi - (B+\lambda)^{-1}B\varphi\\ =&(B_M+\lambda)^{-1}B_M\varphi - (B_M+\lambda)^{-1}B\varphi + (B_M+\lambda)^{-1}B\varphi - (B+\lambda)^{-1}B\varphi.\end{aligned}$$

Since $\|(B_M+\lambda)^{-1}\|_{\mathcal{H}_K} \leq \frac{1}{\lambda}$, we have that

$$\|(B_M+\lambda)^{-1}B_M\varphi - (B_M+\lambda)^{-1}B\varphi\|_{\mathcal{H}_K} \leq \frac{1}{\lambda}\|B_M\varphi - B\varphi\|_{\mathcal{H}_K}.$$

Applying Lemma 22 to $B_M\varphi - B\varphi$, we obtain with probability at least $1-\delta/2$

$$\begin{aligned}\frac{1}{\lambda}\|B_M\varphi - B\varphi\|_{\mathcal{H}_K} &\leq \frac{4\kappa R^2\|\varphi\|_\infty\log(4/\delta)}{\lambda M} + \kappa R\|\varphi\|_{L^2(\tilde{\rho}_T^L)}\sqrt{\frac{2\log(4/\delta)}{\lambda^2 M}}\\ &\leq \frac{4\kappa R^2\|\varphi\|_\infty\log(4/\delta)}{\lambda M} + \kappa R^2\|\varphi\|_\infty\sqrt{\frac{2\log(4/\delta)}{\lambda^2 M}}.\end{aligned}$$

On the other hand, we have

$$\begin{aligned}\|(B_M+\lambda)^{-1}B\varphi - (B+\lambda)^{-1}B\varphi\|_{\mathcal{H}_K} &= \|(B_M+\lambda)^{-1}(B-B_M)(B+\lambda)^{-1}B\varphi\|_{\mathcal{H}_K}\\ &\leq \frac{1}{\lambda}\|(B-B_M)(B+\lambda)^{-1}B\varphi\|_{\mathcal{H}_K}.\end{aligned}$$

Since $\varphi_{\mathcal{H}_K}^{\lambda,\infty} = (B+\lambda)^{-1}B\varphi$ is the unique minimizer of the expected risk functional $\mathcal{E}(\psi) = \|A\psi - A\varphi\|_{L^2(\rho_{\boldsymbol{X}})}^2 + \lambda\|\psi\|_{\mathcal{H}_K}^2$, plugging $\psi = 0$, we obtain that

$$\|A\varphi_{\mathcal{H}_K}^{\lambda,\infty} - A\varphi\|_{L^2(\rho_{\boldsymbol{X}})}^2 + \lambda\|\varphi_{\mathcal{H}_K}^{\lambda,\infty}\|_{\mathcal{H}_K}^2 < \|A\varphi\|_{L^2(\rho_{\boldsymbol{X}})}^2,$$

which implies that

$$\|\varphi_{\mathcal{H}_K}^{\lambda,\infty}\|_{\mathcal{H}_K} \leq \frac{1}{\sqrt{\lambda}}\|A\varphi\|_{L^2(\rho_{\boldsymbol{X}})}, \tag{94}$$

$$\|A\varphi_{\mathcal{H}_K}^{\lambda,\infty}\|_{L^2(\rho_{\boldsymbol{X}})}^2 \leq 2\|A\varphi\|_{L^2(\rho_{\boldsymbol{X}})}^2. \tag{95}$$

By Lemma 8 and (94), it follows that

$$\|\varphi_{\mathcal{H}_K}^{\lambda,\infty}\|_\infty \leq \kappa\|\varphi_{\mathcal{H}_K}^{\lambda,\infty}\|_{\mathcal{H}_K} \leq \frac{\kappa}{\sqrt{\lambda}}\|A\varphi\|_{L^2(\rho_{\boldsymbol{X}})}. \tag{96}$$

Suppose the coercivity condition (55) holds. We have that

$$\|\varphi_{\mathcal{H}_K}^{\lambda,\infty}\|_{L^2(\tilde{\rho}_T^L)}^2 \leq \frac{1}{c_{\mathcal{H}_K}}\|A\varphi_{\mathcal{H}_K}^{\lambda,\infty}\|_{L^2(\rho_{\boldsymbol{X}})}^2 \leq \frac{2}{c_{\mathcal{H}_K}}\|A\varphi\|_{L^2(\rho_{\boldsymbol{X}})}^2. \tag{97}$$

Note that $\|A\varphi\|_{L^2(\rho_{\boldsymbol{X}})}^2 < R^2\|\varphi\|_\infty^2$ (see (50)). Applying Lemma 22 to $\varphi_{\mathcal{H}_K}^{\lambda,\infty} = (B+\lambda)^{-1}B\varphi$, and using (96) and (97) , we obtain that with probability at least $1-\delta/2$,

$$\begin{aligned}
\frac{1}{\lambda}\|(B-B_M)(B+\lambda)^{-1}B\varphi\|_{\mathcal{H}_K} &\leq \frac{4\kappa R^2\|\varphi_{\mathcal{H}_K}^{\lambda,\infty}\|_\infty \log(4/\delta)}{\lambda M} + \kappa R\|\varphi_{\mathcal{H}_K}^{\lambda,\infty}\|_{L^2(\tilde{\rho}_T^L)}\sqrt{\frac{2\log(4/\delta)}{\lambda^2 M}} \\
&\leq \frac{4\kappa^2 R^3\|\varphi\|_\infty \log(4/\delta)}{\lambda^{\frac{3}{2}} M} + \frac{\sqrt{2}}{\sqrt{c_{\mathcal{H}_K}}}\kappa^2 R\|\varphi\|_{L^2(\tilde{\rho}_T^L)}\sqrt{\frac{2\log(4/\delta)}{\lambda^2 M}} \\
&\leq \frac{4\kappa^2 R^3\|\varphi\|_\infty \log(4/\delta)}{\lambda^{\frac{3}{2}} M} + \frac{\sqrt{2}}{\sqrt{c_{\mathcal{H}_K}}}\kappa^2 R^2\|\varphi\|_\infty\sqrt{\frac{2\log(4/\delta)}{\lambda^2 M}}.
\end{aligned}$$

Finally, by combining two bounds, we obtain that with a probability at least $1-\delta$

$$\begin{aligned}
&\|(B_M+\lambda)^{-1}B_M\varphi - (B_M+\lambda)^{-1}B\varphi\|_{\mathcal{H}_K} \\
&\leq \frac{\kappa R^2\|\varphi\|_\infty\sqrt{2\log(4/\delta)}}{\sqrt{M}\lambda}\left[(\kappa+1)\sqrt{\frac{2}{c_{\mathcal{H}_K}}} + \frac{(\kappa R+\sqrt{\lambda})\sqrt{2\log(4/\delta)}}{\sqrt{M\lambda}}\right] \\
&\leq \frac{\kappa R^2\|\varphi\|_\infty\sqrt{2\log(4/\delta)}}{\sqrt{M}\lambda}(C_{\kappa,\mathcal{H}_K} + \frac{C_{\kappa,R,\lambda}\sqrt{2\log(4/\delta)}}{\sqrt{M\lambda}}).
\end{aligned}$$

where $C_{\kappa,\mathcal{H}_K} = (\kappa+1)\sqrt{\frac{2}{c_{\mathcal{H}_K}}}$ and $C_{\kappa,R,\lambda} = \kappa R + \sqrt{\lambda}$. □

Proof of Theorem 24. We decompose $\phi_{\mathcal{H}_K}^{\lambda,M} - \phi_{\mathcal{H}_K}^{\lambda,\infty} = \phi_{\mathcal{H}_K}^{\lambda,M} - \tilde{\phi}_{\mathcal{H}_K}^{\lambda,M} + \tilde{\phi}_{\mathcal{H}_K}^{\lambda,M} - \phi_{\mathcal{H}_K}^{\lambda,\infty}$ where $\tilde{\phi}_{\mathcal{H}_K}^{\lambda,M}$ is the empirical minimizer for noise-free observations. Then applying Lemma 22 to the term $\tilde{\phi}_{\mathcal{H}_K}^{\lambda,M} - \phi_{\mathcal{H}_K}^{\lambda,\infty}$, we obtain that with probability at least $1-\delta$,

$$\|\tilde{\phi}_{\mathcal{H}_K}^{\lambda,M} - \phi_{\mathcal{H}_K}^{\lambda,\infty}\|_{\mathcal{H}_K} \leq \frac{\kappa R^2\|\phi\|_\infty\sqrt{2\log(4/\delta)}}{\sqrt{M}\lambda}(C_{\kappa,\mathcal{H}_K} + \frac{C_{\kappa,R,\lambda}\sqrt{2\log(4/\delta)}}{\sqrt{M\lambda}}). \tag{98}$$

We now just need to estimate the "noise part" $\phi_{\mathcal{H}_K}^{\lambda,M} - \tilde{\phi}_{\mathcal{H}_K}^{\lambda,M}$. According to (77),

$$\tilde{\phi}_{\mathcal{H}_K}^{\lambda,M} - \phi_{\mathcal{H}_K}^{\lambda,M} = (B_M+\lambda)^{-1}A_M^*\mathbb{W}_M, \tag{99}$$

where the noise vector $\mathbb{W}_M$ follows a multivariate Gaussian distribution with zero mean and variance $\sigma^2 I_{dNML}$. Note that

$$\begin{aligned}
\|\tilde{\phi}_{\mathcal{H}_K}^{\lambda,M} - \phi_{\mathcal{H}_K}^{\lambda,M}\|_{\mathcal{H}_K}^2 &= \langle \mathbb{W}_M, A_M(B_M+\lambda)^{-2}A_M^*\mathbb{W}_M\rangle \\
&= \mathbb{W}_M^T\Sigma_M\mathbb{W}_M,
\end{aligned}$$

where the matrix

$$\Sigma_M = (K_{\mathbf{f}_\phi}(\mathbb{X}_M,\mathbb{X}_M) + \lambda NdMLI)^{-1}K_{\mathbf{f}_\phi}(\mathbb{X}_M,\mathbb{X}_M)(K_{\mathbf{f}_\phi}(\mathbb{X}_M,\mathbb{X}_M) + \lambda dNMLI)^{-1}.$$

The matrix Σ_M is the matrix form of the operator $A_M(B_M+\lambda)^{-2}A_M^*$, as is derived from (77), (71) and (75). We have that

$$\begin{aligned}\mathrm{Tr}(\Sigma_M) &\le \frac{1}{\lambda^2(MLNd)^2}\mathrm{Tr}(K_{\mathbf{f}_\phi}(\mathbb{X}_M,\mathbb{X}_M))\\ &= \frac{1}{\lambda^2(MLNd)^2}\sum_{m=1,l=1,i=1}^{M,L,N}\frac{1}{N^2}\sum_{k\neq i,k'\neq i}K(r_{ik}^{(m,l)},r_{ik'}^{(m,l)})(\boldsymbol{r}_{ik'}^{(m,l)})^T\boldsymbol{r}_{ik}^{(m,l)}\\ &\le \frac{1}{\lambda^2 d^2 MLN}\kappa^2R^2, a.s.\end{aligned}$$

and

$$\begin{aligned}\mathrm{Tr}(\Sigma_M^2) &\le \frac{1}{\lambda^4(MLNd)^4}\mathrm{Tr}(K_{\mathbf{f}_\phi}(\mathbb{X}_M,\mathbb{X}_M)^2)\\ &= \frac{1}{\lambda^4(MLNd)^4}\sum_{m,m'=1,l,l'=1,i,i'=1}^{M,L,N}\left\|\frac{1}{N^2}\sum_{k\neq i,k'\neq i'}K(r_{ik}^{(m,l)},r_{i'k'}^{(m',l')})\boldsymbol{r}_{ik}^{(m,l)}(\boldsymbol{r}_{i'k'}^{(m',l')})^T\right\|_F^2\\ &\le \frac{\kappa^4R^4}{\lambda^4d^4(MLN)^2}, a.s.\end{aligned}$$

Now we apply the Hanson-Wright inequality (Theorem 30) for the Gaussian random vector $\mathbb{W}_M$ with $S_0=\sigma^2$. Note that for any $\epsilon>0$,

$$\min\left\{\frac{\epsilon^2}{\sigma^4\|\Sigma_M\|_{\mathrm{HS}}^2},\frac{\epsilon}{\sigma^2\|\Sigma_M\|}\right\}\ge\min\left\{\frac{\epsilon^2}{\sigma^4\mathrm{Tr}(\Sigma_M^2)},\frac{\epsilon}{\sigma^2\mathrm{Tr}(\Sigma_M)}\right\},$$

we obtain that, with a probability at least $1-e^{-t^2}$,

$$\begin{aligned}\mathbb{W}_M^T\Sigma_M\mathbb{W}_M &\le \frac{1}{c}\sigma^2\max\{\mathrm{Tr}(\Sigma_M),\sqrt{\mathrm{Tr}(\Sigma_M^2)}\}(1+2t+t^2)\\ &\le \frac{\kappa^2R^2\sigma^2}{c\lambda^2d^2MLN}(1+2t+t^2)\end{aligned}$$

for any $t>0$, where c is an absolute positive constant appearing in the Hanson-Wright inequality. Therefore, with a probability at least $1-\delta$, there holds

$$\|\tilde{\phi}_{\mathcal{H}_K}^{\lambda,M}-\phi_{\mathcal{H}_K}^{\lambda,M}\|_{\mathcal{H}_K}\le\frac{\kappa R\sigma(\log(1/\delta)+1)}{\sqrt{c}\lambda d\sqrt{MLN}}<\frac{2\kappa R\sigma\log(4/\delta)}{\sqrt{c}\lambda d\sqrt{MLN}}. \tag{100}$$

Now combining (98) and (100), we obtain that with probability at least $1-\delta$,

$$\|\phi_{\mathcal{H}_K}^{\lambda,M}-\phi_{\mathcal{H}_K}^{\lambda,\infty}\|_{\mathcal{H}_K}\le\frac{\kappa R^2\|\phi\|_\infty\sqrt{2\log(8/\delta)}}{\sqrt{M}\lambda}(C_{\kappa,\mathcal{H}_K}+\frac{C_{\kappa,R,\lambda}\sqrt{2\log(8/\delta)}}{\sqrt{M\lambda}})+\frac{2\kappa R\sigma\log(8/\delta)}{\sqrt{c}\lambda d\sqrt{MLN}}.$$

□

B Auxiliary lemmas and theorems

Lemma 27. *Let $\boldsymbol{x}$ and $\boldsymbol{y}$ be jointly Gaussian random vectors*

$$\begin{bmatrix}\boldsymbol{x}\\ \boldsymbol{y}\end{bmatrix}\sim\mathcal{N}(\begin{bmatrix}\mu_{\boldsymbol{x}}\\ \mu_{\boldsymbol{y}}\end{bmatrix},\begin{bmatrix}A & C\\ C^T & B\end{bmatrix}), \tag{101}$$

then the marginal distribution of $\boldsymbol{x}$ and the conditional distribution of $\boldsymbol{x}$ given $\boldsymbol{y}$ are

$$\boldsymbol{x}\sim\mathcal{N}(\mu_{\boldsymbol{x}},A),\quad \textit{and } \boldsymbol{x}|\boldsymbol{y}\sim\mathcal{N}(\mu_{\boldsymbol{x}}+CB^{-1}(\boldsymbol{y}-\mu_{\boldsymbol{y}}),A-CB^{-1}C^T). \tag{102}$$

Proof. See, e.g. (Williams and Rasmussen, 2006), Appendix A. □

Lemma 28. *For any function $\varphi \in L^2(\tilde{\rho}_T^L)$, we have that*

$$\|\mathbf{f}_\varphi\|^2_{L^2(\rho_{\boldsymbol{X}})} \leq \frac{N-1}{N}\|\varphi\|^2_{L^2(\tilde{\rho}_T^L)}. \tag{103}$$

Proof. See the proof of Proposition 16 in (Lu et al., 2021) by taking $K = 1$. □

Lemma 29 (Lemma 8 in (De Vito et al., 2005))**.** *Let $\mathcal{H}$ be a Hilbert space and ξ be a random variable on (Z, ρ) with values in $\mathcal{H}$. Suppose that, $\|\xi\|_{\mathcal{H}} \leq S < \infty$ almost surely. Let z_m be i.i.d drawn from ρ. For any $0 < \delta < 1$, with confidence $1 - \delta$,*

$$\left\| \frac{1}{M}\sum_{m=1}^{M}(\xi(z_m) - \mathbb{E}(\xi)) \right\| \leq \frac{4S\log(2/\delta)}{M} + \sqrt{\frac{2\mathbb{E}(\|\xi\|_H^2)\log(2/\delta)}{M}}.$$

The original version of Lemma 29 is presented in (Yurinsky, 1995).

Theorem 30 (Hanson-Wright inequality (Rudelson et al., 2013))**.** *Let $X = (X_1, \cdots, X_n) \in \mathbb{R}^n$ be a random vector with independent components X_i which satisfy $\mathbb{E}X_i = 0$ and $\|X_i\|_{\psi_2} \leq S_0$, where $\|\cdot\|_{\psi_2}$ is the subGaussian norm. Let A be an $n \times n$ matrix and $\|A\|_{HS}$ denote the Hilbert-Schmidt norm. Then, for every $\epsilon \geq 0$*

$$\mathbb{P}\left\{ \left\| X^T A X - \mathbb{E}X^T A X \right\| \geq \epsilon \right\} \leq 2\exp\left\{ -c\min\left\{ \frac{\epsilon^2}{S_0^4\|A\|_{HS}^2}, \frac{\epsilon}{S_0^2\|A\|} \right\} \right\},$$

where c is an absolute positive constant.

Reference

Ames, W. F. and Pachpatte, B. (1997). Inequalities for differential and integral equations, volume 197. Elsevier.

Archambeau, C., Cornford, D., Opper, M., and Shawe-Taylor, J. (2007). Gaussian process approximations of stochastic differential equations. In Gaussian Processes in Practice, pages 1–16. PMLR.

Bauer, F., Pereverzev, S., and Rosasco, L. (2007). On regularization algorithms in learning theory. Journal of complexity, 23(1):52–72.

Baumann, F., Sokolov, I. M., and Tyloo, M. (2020). A laplacian approach to stubborn agents and their role in opinion formation on influence networks. Physica A: Statistical Mechanics and its Applications, 557:124869.

Bhatia, R. (2013). Matrix analysis, volume 169. Springer Science & Business Media.

Bishwal, J. P. N. et al. (2011). Estimation in interacting diffusions: Continuous and discrete sampling. Applied Mathematics, 2(9):1154–1158.

Blanchard, G. and Mücke, N. (2018). Optimal rates for regularization of statistical inverse learning problems. Foundations of Computational Mathematics, 18(4):971–1013.

Blank, J., Exner, P., and Havlicek, M. (2008). Hilbert space operators in quantum physics. Springer Science & Business Media.

Bongini, M., Fornasier, M., Hansen, M., and Maggioni, M. (2017). Inferring interaction rules from observations of evolutive systems i: The variational approach. Mathematical Models and Methods in Applied Sciences, 27(05):909–951.

Brunton, S. L., Proctor, J. L., and Kutz, J. N. (2016). Discovering governing equations from data by sparse identification of nonlinear dynamical systems. Proceedings of the national academy of sciences, 113(15):3932–3937.

Caponnetto, A. and De Vito, E. (2005). Fast rates for regularized least-squares algorithm. Technical report, MIT.

Chen, J., Kang, L., and Lin, G. (2020). Gaussian process assisted active learning of physical laws. Technometrics, pages 1–14.

Chen, X. (2021). Maximum likelihood estimation of potential energy in interacting particle systems from single-trajectory data. Electronic Communications in Probability, 26:1–13.

Chen, Y., Hosseini, B., Owhadi, H., and Stuart, A. M. (2021). Solving and learning nonlinear pdes with gaussian processes. arXiv preprint arXiv:2103.12959.

Chuang, Y.-L., D'Orsogna, M. R., Marthaler, D., Bertozzi, A. L., and Chayes, L. S. (2007). State transitions and the continuum limit for a 2d interacting, self-propelled particle system. Physica D: Nonlinear Phenomena, 232(1):33–47.

Cohn, D. A., Ghahramani, Z., and Jordan, M. I. (1996). Active learning with statistical models. Journal of artificial intelligence research, 4:129–145.

Cucker, F. and Smale, S. (2002). On the mathematical foundations of learning. Bulletin of the American Mathematical Society, 39:1–49.

De Vito, E., Rosasco, L., Caponnetto, A., De Giovannini, U., Odone, F., and Bartlett, P. (2005). Learning from examples as an inverse problem. Journal of Machine Learning Research, 6(5).

Della Maestra, L. and Hoffmann, M. (2022). The lan property for mckean-vlasov models in a mean-field regime. arXiv preprint arXiv:2205.05932.

Devroye, L., Györfi, L., and Lugosi, G. (2013). A probabilistic theory of pattern recognition, volume 31. Springer Science & Business Media.

D'Orsogna, M. R., Chuang, Y.-L., Bertozzi, A. L., and Chayes, L. S. (2006). Self-propelled particles with soft-core interactions: patterns, stability, and collapse. Physical review letters, 96(10):104302.

Engle, M. H. H. and Neubauer, A. (1996). Regularization of inverse problems, volume 375 of mathematics and its applications.

Genon-Catalot, V. and Larédo, C. (2022). Inference for ergodic mckean-vlasov stochastic differential equations with polynomial interactions. hal-03866218v2.

Gomes, S. N., Stuart, A. M., and Wolfram, M.-T. (2019). Parameter estimation for macroscopic pedestrian dynamics models from microscopic data. SIAM Journal on Applied Mathematics, 79(4):1475–1500.

Gu, M., Liu, X., Fang, X., and Tang, S. (2022). Scalable marginalization of latent variables for correlated data. arXiv preprint arXiv:2203.08389.

Györfi, L., Kohler, M., Krzyzak, A., and Walk, H. (2006). A distribution-free theory of nonparametric regression. Springer Science & Business Media.

Heinonen, M., Yildiz, C., Mannerström, H., Intosalmi, J., and Lähdesmäki, H. (2018). Learning unknown ode models with gaussian processes. In International Conference on Machine Learning, pages 1959–1968. PMLR.

Kasonga, R. A. (1990). Maximum likelihood theory for large interacting systems. SIAM Journal on Applied Mathematics, 50(3):865–875.

Lee, S., Kooshkbaghi, M., Spiliotis, K., Siettos, C. I., and Kevrekidis, I. G. (2020). Coarse-scale pdes from fine-scale observations via machine learning. Chaos: An Interdisciplinary Journal of Nonlinear Science, 30(1):013141.

Li, Z., Zheng, H., Kovachki, N., Jin, D., Chen, H., Liu, B., Azizzadenesheli, K., and Anandkumar, A. (2021). Physics-informed neural operator for learning partial differential equations. arXiv preprint arXiv:2111.03794.

Liu, D. C. and Nocedal, J. (1989). On the limited memory bfgs method for large scale optimization. Mathematical programming, 45(1):503–528.

Liu, Q. (2017). Stein variational gradient descent as gradient flow. In Guyon, I., Luxburg, U. V., Bengio, S., Wallach, H., Fergus, R., Vishwanathan, S., and Garnett, R., editors, Advances in Neural Information Processing Systems, volume 30. Curran Associates, Inc.

Long, Z., Lu, Y., Ma, X., and Dong, B. (2018). Pde-net: Learning pdes from data. In International Conference on Machine Learning, pages 3208–3216. PMLR.

Lu, F., Maggioni, M., and Tang, S. (2020). Learning interaction kernels in stochastic systems of interacting particles from multiple trajectories. arXiv preprint arXiv:2007.15174.

Lu, F., Maggioni, M., and Tang, S. (2021). Learning interaction kernels in heterogeneous systems of agents from multiple trajectories. Journal of Machine Learning Research, 22(32):1–67.

Lu, F., Zhong, M., Tang, S., and Maggioni, M. (2019). Nonparametric inference of interaction laws in systems of agents from trajectory data. Proceedings of the National Academy of Sciences, 116(29):14424–14433.

Mao, Z., Li, Z., and Karniadakis, G. E. (2019). Nonlocal flocking dynamics: Learning the fractional order of pdes from particle simulations. Communications on Applied Mathematics and Computation, 1(4):597–619.

Mei, S., Montanari, A., and Nguyen, P.-M. (2018). A mean field view of the landscape of two-layer neural networks. Proceedings of the National Academy of Sciences, 115(33):E7665–E7671.

Messenger, D. A. and Bortz, D. M. (2021). Learning mean-field equations from particle data using wsindy. arXiv preprint arXiv:2110.07756.

Messenger, D. A., Wheeler, G. E., Liu, X., and Bortz, D. M. (2022). Learning anisotropic interaction rules from individual trajectories in a heterogeneous cellular population. arXiv preprint arXiv:2204.14141.

Miller, J., Tang, S., Zhong, M., and Maggioni, M. (2020). Learning theory for inferring interaction kernels in second-order interacting agent systems. arXiv preprint arXiv:2010.03729.

Motsch, S. and Tadmor, E. (2014). Heterophilious dynamics enhances consensus. SIAM review, 56(4):577–621.

Qin, T., Wu, K., and Xiu, D. (2019). Data driven governing equations approximation using deep neural networks. Journal of Computational Physics.

Quinonero-Candela, J. and Rasmussen, C. E. (2005). A unifying view of sparse approximate gaussian process regression. The Journal of Machine Learning Research, 6:1939–1959.

Raissi, M. (2018). Deep hidden physics models: Deep learning of nonlinear partial differential equations. The Journal of Machine Learning Research, 19(1):932–955.

Raissi, M., Perdikaris, P., and Karniadakis, G. (2018). Multistep neural networks for data-driven discovery of nonlinear dynamical systems. arXiv preprint arXiv:1801.01236.

Raissi, M., Perdikaris, P., and Karniadakis, G. E. (2017). Machine learning of linear differential equations using gaussian processes. Journal of Computational Physics, 348:683–693.

Rudelson, M., Vershynin, R., et al. (2013). Hanson-wright inequality and sub-gaussian concentration. Electronic Communications in Probability, 18.

Schäfer, F., Katzfuss, M., and Owhadi, H. (2021). Sparse cholesky factorization by kullback–leibler minimization. SIAM Journal on Scientific Computing, 43(3):A2019–A2046.

Sharrock, L., Kantas, N., Parpas, P., and Pavliotis, G. A. (2021). Parameter estimation for the mckean-vlasov stochastic differential equation. arXiv preprint arXiv:2106.13751.

Smale, S. and Zhou, D.-X. (2007). Learning theory estimates via integral operators and their approximations. Constructive approximation, 26(2):153–172.

Stepaniants, G. (2021). Learning partial differential equations in reproducing kernel hilbert spaces. arXiv preprint arXiv:2108.11580.

Tang, W., Zhang, L., and Banerjee, S. (2021). On identifiability and consistency of the nugget in gaussian spatial process models. arXiv preprint arXiv:1908.05726.

Taylor, M. (1968). Towards a mathematical theory of influence and attitude change. Human Relations, 21(2):121–139.

Wang, H. and Zhou, X. (2021). Explicit estimation of derivatives from data and differential equations by gaussian process regression. International Journal for Uncertainty Quantification, 11(4).

Wang, S., Wang, H., and Perdikaris, P. (2021). Learning the solution operator of parametric partial differential equations with physics-informed deeponets. arXiv preprint arXiv:2103.10974.

Williams, C. K. and Rasmussen, C. E. (2006). Gaussian processes for machine learning, volume 2. MIT press Cambridge, MA.

Yang, S., Wong, S. W., and Kou, S. (2021). Inference of dynamic systems from noisy and sparse data via manifold-constrained gaussian processes. Proceedings of the National Academy of Sciences, 118(15).

Yao, R., Chen, X., and Yang, Y. (2022). Mean-field nonparametric estimation of interacting particle systems. arXiv preprint arXiv:2205.07937.

Yildiz, C., Heinonen, M., Intosalmi, J., Mannerstrom, H., and Lahdesmaki, H. (2018). Learning stochastic differential equations with gaussian processes without gradient matching. In 2018 IEEE 28th International Workshop on Machine Learning for Signal Processing (MLSP), pages 1–6. IEEE.

Yurinsky, V. (1995). Sums and Gaussian Vectors. Lecture Notes in Mathematics. Springer Berlin, Heidelberg.

Zhang, H. (2004). Inconsistent estimation and asymptotically equal interpolations in model-based geostatistics. Journal of the American Statistical Association, 99(465):250–261.

Zhao, Z., Tronarp, F., Hostettler, R., and Särkkä, S. (2020). State-space gaussian process for drift estimation in stochastic differential equations. In ICASSP 2020-2020 IEEE International Conference on Acoustics, Speech and Signal Processing (ICASSP), pages 5295–5299. IEEE.

Zhong, M., Miller, J., and Maggioni, M. (2020). Data-driven discovery of emergent behaviors in collective dynamics. Physica D: Nonlinear Phenomena, 411:132542.